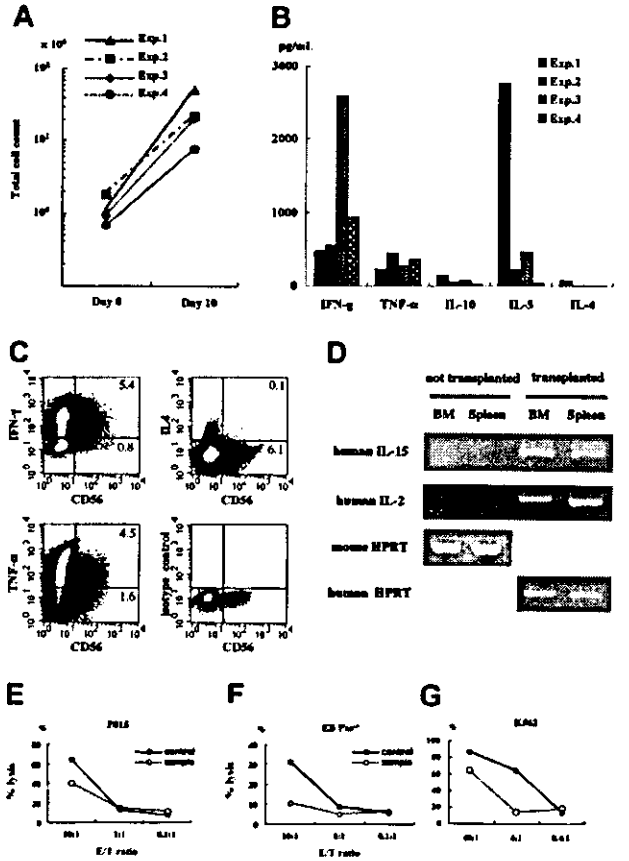

Figure 6. Functional analysis of human lymphocytes in spleen of NOD/SCID/γ_c^{null} mice. Four to 6 months after the transplantation of 2 × 10^4 to 5 × 10^4 CB CD34$^+$ cells, human lymphocytes in spleen were cultured and expanded for functional analyses. (A) Cell proliferation after 10-day culture; PHA (1 μg/mL) and hIL-2 (50 IU/mL) for the initial 48 hours followed by hIL-2 (50 IU/mL) only for 8 days. (B) Supernatants of the spleen cells after 48-hour stimulation with PHA and hIL-2 were taken, and the production of human cytokines was evaluated using Cytometric Bead Array Kit for human cytokine (BD PharMingen). (C) PHA-stimulated human lymphocytes were further stimulated with 10 ng/mL PMA and 1 μg/mL ionomycin for 6 hours. Brefeldin A was added during the last 2 hours. Then the cells were stained with membrane CD56 and intracellular cytokines and were analyzed using flow cytometry. (D) RNA was isolated from the spleen and BM of NOD/SCID/γ_c^{null} mice with or without transplanted CD34$^+$ cells, and the expression of mRNA for human IL-2 and IL-15 was examined by RT-PCR. Human or mouse HPRT was used as a positive control. (E-G) Anti–CD3-dependent cytotoxic T-lymphocyte activity and NK activity were evaluated by measuring the release of calcine-AM into the supernatant after cytolysis of target cells labeled with calcine. Results are expressed as the percentage of specific lysis. PB MNCs of a healthy adult were used as a positive control. Representative data with similar results of 4 independent experiments are shown.

reported that IL-2 and IL-15 are essential to the development and maintenance of NK cells.[22,23] Therefore, we also examined the production of these cytokines by reverse transcription–polymerase chain reaction (RT-PCR) and identified them in the spleen and BM of NOD/SCID/γ_c^{null} mice with transplanted CD34$^+$ (Figure 6D).

Further, these T cells exerted cell-mediated cytotoxicity. Fas + perforin-dependent or perforin-dependent cytotoxicity was evaluated using P815 cells or the Fas-deficient Epstein-Barr virus–transformed B-cell line (Fas$^{-/-}$ EB) as target cells, respectively. Fas + perforin-dependent cytotoxicity was comparable but a little lower than in a healthy adult human (Figure 6E). Cytotoxic activity dependent solely on the perforin-mediated pathway was lower than in control (Figure 6F). Although the value was not enough to be statistically significant, the percentage lysis of Fas$^{-/-}$ EB cells by samples always surpassed those of negative controls (typically less than 5% and never more than 10%), which are the ones with isotype control mAb or without antibody. Further investigation will be needed to clarify the pathway involved in the killing by these cells. Natural killer activity was evaluated using K562 cells, which are commonly used for the assessment of NK cell activity.[24] As shown in Figure 6G, human mononuclear cells in the spleens of NOD/SCID/γ_c^{null} mice showed substantial levels of cytotoxicity against K562 cells, suggesting that human NK cells functionally matured. However, to exclude the possibility that coexisting other cells, such as T cells in the test sample, might contribute to K562 cell killing, we performed the same experiments with human CD56-depleted splenocytes as effector cells. Human CD56 depletion abrogated K562 cell killing almost completely (99.8% ± 0.03% inhibition; n = 3), which clearly demonstrated that the lysis of K562 cells was attributable to NK cells.

Histologic evaluation of reconstituted lymphoid organs

Lymphoid organs in NOD/SCID/γ_c^{null} mice that received transplanted human CD34$^+$ CB cells were examined histologically 5 months after transplantation (Figure 7). Although the thymus of the recipient mouse was highly atrophic, human CD45$^+$ cells were identified, usually as CD3$^+$ T cells. These T cells were predominantly CD4$^+$CD8$^+$ DP T cells and were positive for human CD1a$^+$, which is expressed on immature thymocytes. These cells were also positive for the cell-cycle–specific antigen Ki-67. Cytokeratin staining revealed the presence of an epithelial cell network inside the thymus, and these epithelial cells were positive for major histocompatibility complex class 2 (MHC class 2) of NOD mice (data not shown). These findings suggested that the immature human T cells that resided in the epithelial network were of mouse origin. In the spleen, a mononuclear cell-rich region similar to

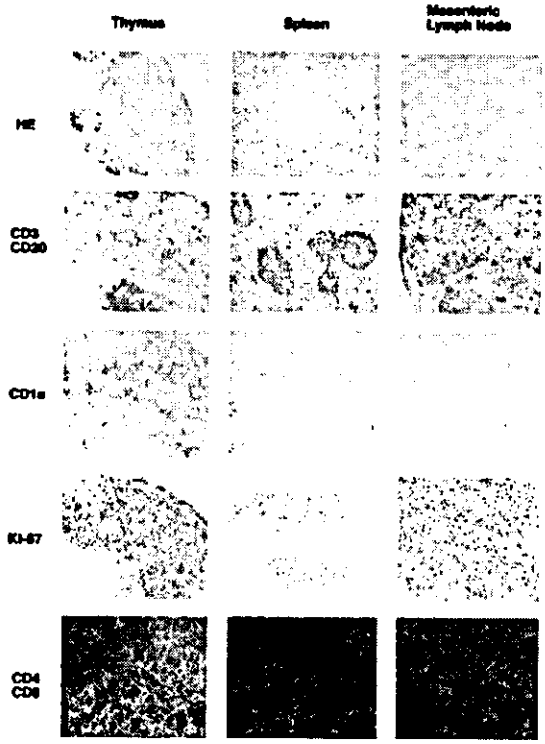

Figure 7. Immunohistochemical staining of the thymus, spleen, and mesenteric lymph nodes. Six months after transplantation, various organs were taken, and frozen sections were prepared. Expressions of human CD3 (Vector Blue)/human CD20 (DAB), human CD1a (Vector Blue), human Ki-67 (Vector Blue), and human CD4 (Alexa 488)/human CD8 (Cy3) were evaluated. Original magnification is × 400 for CD4/CD8 images, × 100 for all others.

white pulp appeared after transplantation. This structure was never found in NOD/SCID/γ_c^{null} mice that did not undergo transplantation. Antihuman CD45 staining showed that the cell-rich region consisted mainly of human hematopoietic cells. Antihuman CD3 and CD20 double staining revealed that the structure consisted of human $CD3^+$ cells surrounding a vessel and human $CD20^+$ cells flanking the $CD3^+$-cell–rich region. This structure resembled a periarteriolar lymphoid sheath (PALS) and primary follicles seen in humans. Mesenteric lymph nodes in NOD/SCID/γ_c^{null} mice with transplanted CB $CD34^+$ cells also consisted mainly of human $CD3^+$ cells. Double staining with CD3 and CD20 revealed that this tissue was densely engrafted with human T and B cells but devoid of typical follicular structures. These findings indicated that organized structures of the thymus, spleen, and mesenteric lymph nodes were reconstituted to a considerable extent by human-derived lymphocytes in NOD/SCIDγ_c^{null} mice.

Discussion

Development and functional maturation of human lymphocytes are achieved through complex networks in various organs, such as BM, thymus, spleen, and lymph node. Many attempts have been made to reconstitute a functional human immune system in mice with the *scid* phenotype but have resulted in limited success.[1-3,25-27] We obtained evidence for the reconstitution of functional T cells, B cells, and NK cells from CB $CD34^+$ cells in NOD/SCID/γ_c^{null} mice without the cotransplantation of human tissues. After the transplantation of CB $CD34^+$ cells, all classes of human lymphocytes were invariably identified. T-cell development and maturation levels in these mice were similar to those in humans. The thymus contained immature T cells of DP and DN phenotypes, and the spleen was rich in mature SP T cells. $CD3^+CD45^+$ naive T cells were generated to an extent comparable to that in humans. The TCR of these T cells was predominantly $\alpha\beta$, but T cells with $\gamma\delta$TCR were also observed in the spleen. Flow-cytometry–based quantification of TCR Vβ (TCRBV) of human $CD3^+$ cells in the spleen showed a divergent repertoire, thus implying acquisition of the potential to respond to highly diverse molecules. Indeed, generated T cells proliferated with PHA stimulation and produced human cytokines. These T blasts showed cell-mediated cytotoxicity, thereby demonstrating the functional maturation of human T cells in a mouse environment. Like T cells, NK cells were mature enough to exert cytotoxicity against K562 cells. B-cell development and maturation levels were also comparable to those in humans. Immature B cells predominantly resided in the BM, and mature surface immunoglobulin-positive B cells were predominant in the spleen. Although human B-cell differentiation can be seen in NOD/SCID mice, only the NOD/SCID/γ_c^{null} mice model enabled human IgM, IgG, and IgA production in mouse serum, which means that the generated human T and B cells were functionally competent. These findings suggest that complicated developmental processes of T and B lymphocytes were reproduced in the NOD/SCID/γ_c^{null} mice model.

In the SCID-hu mouse model, simultaneous implantation of fetal thymus and liver was indispensable for the generation of functionally mature human T cells.[8] In the beige/nude/xid/human (bnx/hu) mice model, human T cells could develop from HSCs through the cotransplantation of genetically altered human BM stromal cells, which produced human cytokines.[28] However, extrathymically developed T cells were functionally impaired. Systemic administration of human IL-7 restored function, but to a limited extent.[9] Considering these findings, NOD/SCID/γ_c^{null} mice seemed to provide an excellent environment for human T-cell development. Contrary to previous models, the NOD/SCID/γ_c^{null} mice model did not require the cotransplantation of human tissue. The interesting question is whether these mice have unique properties for human lymphocyte development or a profound immunodeficiency that enables some kind of human tissue formation. Production of IL-2 and IL-15, which are essential for NK cell development, in these mice after transplantation may suggest that this model can reconstitute the environment required for lymphopoiesis. More detailed identification of engrafted human cells is under investigation. Organized clustering of lymphocytes in appropriate organs is required for the reconstitution of a functional immune system. In NOD/SCID/γ_c^{null} mice with transplanted human CB $CD34^+$ cells, T- and B-cell clustering is seen in the thymus, spleen, and lymph nodes. The thymus was engrafted with immature T cells, whereas the spleen contained mature T cells that formed clusters with B cells. PALS-like structures consisting mainly of human hematopoietic cells were also identified, and these structures were absent before transplantation. In lymph nodes, many T and B cells were identified, but distinct follicular structures were missing. This may reflect that critical molecules for lymphocytes, such as adhesion molecules or chemokines, are not available for human cells in a mouse environment, which could prove an obstacle to analyzing the human immune system in detail.

One important question is how human T cells develop. Human $CD3^-$ T cells with the $CD4^+CD8^+$ DP phenotype in the thymus were positive for human CD1a, which is expressed on immature thymocytes.[29] These cells were also positive for TdT (data not shown) and the cell-cycle–specific antigen Ki-67. Furthermore, cytokeratin staining revealed the presence of an epithelial cell network derived mainly from mice (data not shown). These results strongly suggest that the generation of human T cells occurs in the thymus of NOD/SCID/γ_c^{null} mice. To exclude the possibility that contaminated T cells expanded in mice, we transplanted CB Lin^- $CD34^+$ cells into NOD/SCID/γ_c^{null} mice and performed sequential analysis. T cells first appeared only in the thymus with the phenotype of immature thymocytes, followed by seeding to peripheral organs. This finding supports the notion that human T cells were derived from HSCs, maturated in the mouse thymus, and seeded to the periphery. Another important observation is that as few as 100 $CD34^+$ cells could engraft and give rise to multilineage blood cells in our mice, as we have already reported.[16] Even after the transplantation of these few $CD34^+$ cells, we confirmed the presence of $CD3^+$ cells 5 months after transplantation using flow cytometry. Although our results strongly suggest the generation of human T cells in the mouse thymus, the possibility of extrathymic differentiation must be examined. To clarify the site(s) for T-cell development, the results of thymectomy experiments have to be analyzed. It is also noteworthy that NOD/SCID/γ_c^{null} mice with transplanted human CB $CD34^+$ cells showed almost no appreciable evidence of GVHD responses despite a considerable number of human T cells in these mice. Transfer of human PB lymphocytes into *scid* mice induces a substantial immune response against mouse xenoantigens that skews the human TCR repertoire[30] and induces GVHD.[31,32] The mice died within a few weeks. Under physiological conditions, intrathymic T-cell differentiation is characterized by 2 selection events: positive and negative selection. Two types of molecules produced by nonlymphoid thymic cells—MHC molecules and cytokines—play important roles in T-cell maturation. MHC molecules are indispensable for positive and negative selection, serving to preserve useful cells and to eliminate potentially harmful ones. As for which MHC restriction orchestrates human lymphocyte development, at least 2 possibilities are

likely. One is human MHC. Sanchez et al[33] reported that human CB contains a cell population that supports the differentiation of $CD34^+$ cells into $CD4^+$ or $CD8^+$ naive T cells in serum-deprived cultures. The other possibility is xenogenic mouse MHC. Robin et al[34] and Weekx et al[35] reported the generation of human T-lymphoid progenitor cells from $CD34^+CD38^-$, $CD34^+CD38^{low}$, and $CD34^+CD38^+$ subsets of human CB and BM cells in fetal thymus organ cultures from NOD/SCID or *scid* mice. Zhao et al[36] also showed that normal immune functions and specific T-cell tolerance to discordant xenogenic donors were achieved by grafting fetal pig thymus and liver tissue to T-cell– and NK-cell–depleted thymectomized mice. These 2 possibilities—human MHC and xenogenic mouse MHC—must be examined further to elucidate the mechanism underlying the generation of human T cells in NOD/SCID/γ_c^{null} mice.

Our mouse model is an excellent in vivo model in which to complete the reconstitution of human lymphocytes from HSCs without transplanting additional human tissues. Use of this model will be a unique way to investigate human lymphopoiesis, which has been analyzed in a combination of different assay systems. We conclude that NOD/SCID/γ_c^{null} mice are a potent and versatile species that can be used to analyze human lymphopoiesis and human HSCs.

Acknowledgments

We thank Dr M. Yasukawa for kindly providing the EB $Fas^{-/-}$ cell line, Dr K. Omori (Kyoto University Hospital, Kyoto, Japan) for helpful discussions, and M. Ohara (Fukuoka, Japan) for language assistance.

References

1. McCune JM, Namikawa R, Kaneshima H, Shultz LD, Lieberman M, Weissman IL. The SCID-hu mouse: murine model for the analysis of human hematolymphoid differentiation and function. Science. 1988;241:1632-1639.
2. Mosier DE, Gulizia RJ, Baird SM, Wilson DB. Transfer of a functional human immune system to mice with severe combined immunodeficiency. Nature. 1988;335:256-259.
3. Namikawa R, Weilbaecher KN, Kaneshima H, Yee EJ, McCune JM. Long-term human hematopoiesis in the SCID-hu mouse. J Exp Med. 1990; 172:1055-1063.
4. Lapidot T, Pflumio F, Doedens M, Murdoch B, Williams DE, Dick JE. Cytokine stimulation of multilineage hematopoiesis from immature human cells engrafted in SCID mice. Science. 1992;255: 1137-1141.
5. Kyoizumi S, Baum CM, Kaneshima H, McCune JM, Yee EJ, Namikawa R. Implantation and maintenance of functional human bone marrow in SCID-hu mice. Blood. 1992;79:1704-1711.
6. Carballido JM, Schols D, Namikawa R, et al. IL-4 induces human B cell maturation and IgE synthesis in SCID-hu mice: inhibition of ongoing IgE production by in vivo treatment with an IL-4/IL-13 receptor antagonist. J Immunol. 1995;155:4162-4170.
7. Roncarolo MG, Carballido JM, Rouleau M, Namikawa R, de Vries JE. Human T- and B-cell functions in SCID-hu mice. Semin Immunol. 1996;8: 207-213.
8. Carballido JM, Namikawa R, Carballido-Perrig N, Antonenko S, Roncarolo MG, de Vries JE. Generation of primary antigen-specific human T- and B-cell responses in immunocompetent SCID-hu mice. Nat Med. 2000;6:103-106.
9. Tsark EC, Dao MA, Wang X, Weinberg K, Nolta JA. IL-7 enhances the responsiveness of human T cells that develop in the bone marrow of athymic mice. J Immunol. 2001;166:170-181.
10. Hesselton RM, Greiner DL, Mordes JP, Rajan TV, Sullivan JL, Shultz LD. High levels of human peripheral blood mononuclear cell engraftment and enhanced susceptibility to human immunodeficiency virus type 1 infection in NOD/LtSz-scid/scid mice. J Infect Dis. 1995;172:974-982.
11. Yoshino H, Ueda T, Kawahata M, et al. Natural killer cell depletion by anti-asialo GM1 antiserum treatment enhances human hematopoietic stem cell engraftment in NOD/Shi-scid mice. Bone Marrow Transplant. 2000;26:1211-1216.
12. Ueda T, Tsuji K, Yoshino H, et al. Expansion of human NOD/SCID-repopulating cells by stem cell factor, Flk2/Flt3 ligand, thrombopoietin, IL-6, and soluble IL-6 receptor. J Clin Invest. 2000;105: 1013-1021.
13. Ueda T, Yoshino H, Kobayashi K, et al. Hematopoietic repopulating ability of cord blood CD34(+) cells in NOD/Shi-scid mice. Stem Cells. 2000;18: 204-213.
14. Kollet O, Peled A, Byk T, et al. β2 microglobulin-deficient (B2m(null)) NOD/SCID mice are excellent recipients for studying human stem cell function. Blood. 2000;95:3102-3105.
15. Glimm H, Eisterer W, Lee K, et al. Previously undetected human hematopoietic cell populations with short-term repopulating activity selectively engraft NOD/SCID-β2 microglobulin-null mice. J Clin Invest. 2001;107:199-206.
16. Ito M, Hiramatsu H, Kobayashi K, et al. NOD/SCID/γ(c)(null) mouse: an excellent recipient mouse model for engraftment of human cells. Blood. 2002;100:3175-3182.
17. Noguchi M, Yi H, Rosenblatt HM, et al. Interleukin-2 receptor gamma chain mutation results in X-linked severe combined immunodeficiency in humans. Cell. 1993;73:147-157.
18. Puck JM, Deschenes SM, Porter JC, et al. The interleukin-2 receptor gamma chain maps to Xq13.1 and is mutated in X-linked severe combined immunodeficiency, SCIDX1. Hum Mol Genet. 1993;2:1099-1104.
19. Yahata T, Ando K, Nakamura Y, et al. Functional human T lymphocyte development from cord blood CD34(+) cells in nonobese diabetic/Shi-scid, IL-2 receptor gamma null mice. J Immunol. 2002;169:204-209.
20. Koyanagi Y, Tanaka Y, Kira J, et al. Primary human immunodeficiency virus type 1 viremia and central nervous system invasion in a novel hu-PBL–immunodeficient mouse strain. J Virol. 1997;71:2417-2424.
21. Lichtenfels R, Biddison WE, Schulz H, Vogt AB, Martin R. CARE-LASS (calcine-release-assay), an improved fluorescence-based test system to measure cytotoxic T lymphocyte activity. J Immunol Methods. 1994;172:227-239.
22. Williams NS, Klem J, Puzanov IJ, et al. Natural killer cell differentiation: insights from knockout and transgenic mouse models and in vitro systems. Immunol Rev. 1998;165:47-61.
23. Cooper MA, Bush JE, Fehniger TA, et al. In vivo evidence for a dependence on interleukin 15 for survival of natural killer cells. Blood. 2002;100: 3633-3638.
24. Whiteside TL, Herberman RB. The biology of human natural killer cells. Ann Ist Super Sanita. 1990;26:335-348.
25. Peault B, Weissman IL, Baum C, McCune JM, Tsukamoto A. Lymphoid reconstitution of the human fetal thymus in SCID mice with $CD34^+$ precursor cells. J Exp Med. 1991;174:1283-1286.
26. Kollmann TR, Kim A, Zhuang X, Hachamovitch M, Goldstein H. Reconstitution of SCID mice with human lymphoid and myeloid cells after transplantation with human fetal bone marrow without the requirement for exogenous human cytokines. Proc Natl Acad Sci U S A. 1994;91:8032-8036.
27. Tournoy KG, Depraetere S, Meuleman P, Leroux-Roels G, Pauwels RA. Murine IL-2 receptor beta chain blockade improves human leukocyte engraftment in SCID mice. Eur J Immunol. 1998;28: 3221-3230.
28. Dao MA, Pepper KA, Nolta JA. Long-term cytokine production from engineered primary human stromal cells influences human hematopoiesis in an in vivo xenograft model. Stem Cells. 1997;15: 443-454.
29. Martin LH, Calabi F, Lefebvre FA, Bilsland CA, Milstein C. Structure and expression of the human thymocyte antigens CD1a, CD1b, and CD1c. Proc Natl Acad Sci U S A. 1987;84:9189-9193.
30. Tary-Lehmann M, Lehmann PV, Schols D, Roncarolo MG, Saxon A. Anti-SCID mouse reactivity shapes the human $CD4^+$ T cell repertoire in hu-PBL-SCID chimeras. J Exp Med. 1994;180:1817-1827.
31. Hozumi N, Gorczynski R, Peters W, Sandhu JS. A SCID mouse model for human immune response and disease. Res Immunol. 1994;145: 370-379.
32. Pflumio F, Lapidot T, Murdoch B, Patterson B, Dick JE. Engraftment of human lymphoid cells into newborn SCID mice leads to graft-versus-host disease. Int Immunol. 1993;5:1509-1522.
33. Sanchez M, Alfani E, Visconti G, Passarelli AM, Migliaccio AR, Migliaccio G. Thymus-independent T-cell differentiation in vitro. Br J Haematol. 1998; 103:1198-1205.
34. Robin C, Bennaceur-Griscelli A, Louache F, Vainchenker W, Coulombel L. Identification of human T-lymphoid progenitor cells in $CD34^+$ $CD38^{low}$ and $CD34^+$ $CD38^+$ subsets of human cord blood and bone marrow cells using NOD-SCID fetal thymus organ cultures. Br J Haematol. 1999;104:809-819.
35. Weekx SF, Snoeck HW, Offner F, et al. Generation of T cells from adult human hematopoietic stem cells and progenitors in a fetal thymic organ culture system: stimulation by tumor necrosis factor-α. Blood. 2000;95:2806-2812.
36. Zhao Y, Swenson K, Sergio JJ, Sykes M. Pig MHC mediates positive selection of mouse $CD4^+$ T cells with a mouse MHC-restricted TCR in pig thymus grafts. J Immunol. 1998;161:1320-1326.

Development of both human connective tissue-type and mucosal-type mast cells in mice from hematopoietic stem cells with identical distribution pattern to human body

Naotomo Kambe, Hidefumi Hiramatsu, Mika Shimonaka, Hisanori Fujino, Ryuta Nishikomori, Toshio Heike, Mamoru Ito, Kimio Kobayashi, Yoshito Ueyama, Norihisa Matsuyoshi, Yoshiki Miyachi, and Tatsutoshi Nakahata

The transplantation of primitive human cells into sublethally irradiated immunodeficient mice is the well-established in vivo system for the investigation of human hematopoietic stem cell function. Although mast cells are the progeny of hematopoietic stem cells, human mast cell development in mice that underwent human hematopoietic stem cell transplantation has not been reported. Here we report on human mast cell development after xenotransplantation of human hematopoietic stem cells into nonobese diabetic severe combined immunodeficient (NOD/SCID)/γ_c^{null} (NOG) mice with severe combined immunodeficiency and interleukin 2 (IL-2) receptor γ-chain allelic mutation. Supported by the murine environment, human mast cell clusters developed in mouse dermis, but they required more time than other forms of human cell reconstitution. In lung and gastric tract, mucosal-type mast cells containing tryptase but lacking chymase located on gastric mucosa and in alveoli, whereas connective tissue-type mast cells containing both tryptase and chymase located on gastric submucosa and around major airways, as in the human body. Mast cell development was also observed in lymph nodes, spleen, and peritoneal cavity but not in the peripheral blood. Xenotransplantation of human hematopoietic stem cells into NOG mice can be expected to result in a highly effective model for the investigation of human mast cell development and function in vivo. (Blood. 2004;103: 860-867)

Introduction

Mast cells are recognized as the principal cells which initiate immunoglobulin E (IgE)–dependent immediate hypersensitivity and also as the cells which contribute to innate immunity and tissue remodeling.[1,2] There are 2 phenotypically distinct mast cell subpopulations in rodents: connective tissue-type mast cells (CTMCs) and mucosal-type mast cells (MMCs). These populations differ in location, cell size, staining characteristics, ultrastructure, mediator content, and T-cell dependency.[3] Proliferation of rodent MMCs is dependent on T-cell–derived cytokines,[3,4] whereas that of CTMCs is supported by stem cell factor (SCF). In humans, mast cells are distinguished on the basis of their protease composition,[5,6] MC_{TC} contains tryptase and chymase in its granules and is predominant in skin and intestinal submucosa, like CTMCs in rodents. MC_T also contains tryptase, but lacks chymase, and is predominant in the alveolar wall and gastric mucosa, similar to MMCs in rodents. Human mast cells were reported to develop only under the influence of SCF, but T-cell–derived interleukin 3 (IL-3) has little affect on their differentiation.[7] Recently, human intestinal mast cells were reported to respond to IL-3 by enhancing their growth,[8] but SCF is still an indispensable factor for human mast cells. Mast cells are the progenies of hematopoietic stem cells (HSCs).[9,10] In mice, the progenitor cells capable of becoming mast cells leave the bone marrow and enter the circulation but complete their differentiation into mast cells only after arriving in peripheral tissues such as lung, bowel, and skin.[10,11] Unfortunately, the developmental mechanism of human mast cells remains far less clear, possibly because the lack of an appropriate in vivo assay system.

The transplantation of primitive human cells into immunodeficient C.B-17-Prkdc^{scid} *(scid)*[12,13] and into NOD/LtSz-*scid* or NOD/Shi-*scid* (nonobese diabetic severe combined immunodeficient [NOD/SCID]) mice[14,15] is thought to constitute an appropriate functional in vivo system for human HSCs. However, it has been suggested that residual natural killer (NK) cell activity in NOD/SCID mice might interfere with engraftment.[16,17] Recently, we developed NOD/SCID/γ_c^{null} (NOG) mice by backcrossing IL-2 receptor γ-chain deficient (γ_c^{null}) mice to NOD/Shi-*scid* mice.[18] Compared with NOD/SCID mice treated with anti-NK cell antibody[17] and NOD/SCID/β_2 microglobulin^{null} mice,[19,20] both of which were established for reducing residual NK cell activity, the newly developed NOG mice were superior in terms of efficiencies of human HSC engraftment, because they lack NK cell activity and show reduced interferon γ production from dendritic cells.[18] In addition, human $CD3^+$ T cells can be generated and matured from human HSCs in NOG but not in other mice.[21,22] These results encouraged us to check human mast cell development in NOG

From the Department of Pediatrics and Dermatology, Kyoto University Graduate School of Medicine, Kyoto, Japan; Central Institute for Experimental Animals, Kawasaki, Japan; and the Department of Pathology, Tokai University School of Medicine, Isehara, Japan.

Submitted April 14, 2003; accepted September 17, 2003. Prepublished online as *Blood* First Edition Paper, October 2, 2003; DOI 10.1182/blood-2003-04-1160.

Supported by grant 14770405 (N.K.) and Grant-in-Aid for Creative Scientific Research (S) 13GS0009 (T.N.) from the Ministry of Education, Science, Sports, and Culture, Japan, as well as the Long-Range Research Initiative grant CS05-07 (Y.M.) from the Japan Industry Association.

Reprints: Tatsutoshi Nakahata, Department of Pediatrics, Kyoto University Graduate School of Medicine, 54 Kawahara-cho, Shogoin, Sakyo-ku, Kyoto 606-8507, Japan; e-mail: tnakaha@kuhp.kyoto-u.ac.jp.

The publication costs of this article were defrayed in part by page charge payment. Therefore, and solely to indicate this fact, this article is hereby marked "advertisement" in accordance with 18 U.S.C. section 1734.

mice, even though there are no reports of mast cell development after human HSC transplantation into mice.

This is, therefore, the first report of human mast cell development in mice after transplantation of human HSCs, with NOG mice as recipients. Moreover, development of human mast cells in NOG mice was supported by the murine environment, and, depending on their protease compositions, the distribution of human mast cells was similar to that in the human body.

Materials and methods

Mice, human cell preparation, and xenotransplantation

NOG mice were established at the Central Institute of Experimental Animals (Kawasaki, Japan) by backcrossing γ_c^{null} mice to NOD/Shi-*scid* mice, as reported previously.[18] The mice were shipped to the animal facility of Kyoto University (Kyoto, Japan) and kept under specific pathogen-free conditions in accordance with the facility's guideline.

Human cord blood was collected from healthy full-term deliveries after obtaining informed consent. Mononuclear cells were isolated on Ficoll-Hypaque (Pharmacia, Uppsala, Sweden) after phagocyte depletion with silica (ImmunoBiological Laboratories, Gunma, Japan).[23] $CD34^+$ cell fractions were further isolated by using AutoMACS (Miltenyi Biotec, Bergisch Gladbach, Germany). After the enrichment, assessment of their purity by flow cytometry showed that approximately 95% of the cells were $CD34^+$ cells. In the experiments using lineage-depleted cells ($lin^-/CD34^+$ cells), cord blood mononuclear cells were treated with StemSep (Stem Cell Technologies, Vancouver, Canada), followed by $CD34^+$ selection.

Xenotransplantation of purified human cells into NOG mice was also described previously.[18,21] Mice were irradiated at 8 to 12 weeks of age with 240 cGy. Enriched $CD34^+$ cells (50 000) were injected intravenously through the tail vein. After the transplantation, mice were given sterile water containing prophylactic neomycin sulfate (Invitrogen, Carlsbad, CA). The experimental protocol was approved by the Human Studies Internal Review Board at Kyoto University (no. 322).

Flow cytometry

Human cell development in NOG mice was periodically monitored with a flow cytometer (FACS Calibur; BD Cytometry, San Diego, CA) with fluorescein isothiocyanate (FITC)–conjugated antihuman CD45 monoclonal antibody (mAb) and allo-phycocyanin (APC)–conjugated antimouse CD45 mAb (BD Pharmingen, San Diego, CA), as previously reported.[18,21] The lineage analysis was performed with APC-conjugated antihuman CD45; phycoerythrin (PE)–conjugated anti-CD3, anti-CD33 (BD Pharmingen), and anti-CD203c mAb which recognized both human mast cells and basophils[24,25]; PC5-conjugated anti-CD19, anti-CD56, and anti-Kit (CD117) mAb (Immunotech, Marseille, France); and biotin-conjugated anti-CD123 (IL-3 receptor α-chain) and streptavidin-FITC (BD Pharmingen).

Murine mast cell determination

Tissue samples were frozen in O.C.T. Tissue-Tek compound (Miles Labs, Elkhart, IN) or fixed in 10% buffered formalin or Carnoy solution (60% ethanol, 30% chloroform, and 10% acetic acid). Those sections were stained with acidic toluidine blue. Carnoy fixed preparations were used for safranin-O and Alcian blue staining.

To collect mast cells from the peritoneal cavity, 5 mL prewarmed Hanks balanced salt solution containing 1% fetal calf serum was injected into the mouse peritoneal cavity. The abdomen was gently massaged for 1 minute, after which the peritoneal cavity was carefully opened, and the fluid containing peritoneal cells was collected with a pipette. One part of the collected cell suspension was used for direct counting of living cells, and the remaining cells were used for staining with toluidine blue or with safranin-O and Alcian blue on the cytospin preparations and for cytometry. On the cytospin preparation, a proportion of the positively stained cells among the 200 nucleated cells was determined.

Immunochemistry

To detect human mast cells, acetone-fixed frozen sections were blocked with donkey serum before incubation with antihuman CD45 mAb (Nichirei, Tokyo, Japan) and then incubated with Cy3-conjugated 2nd Ab (Jackson, West Grove, PA), FITC-conjugated avidin bound to mast cells,[26,27] and Hoechst 33342 (Molecular Probes, Eugene, OR). Specificity of avidin binding to mast cells was confirmed with both human and mouse tissue preparations from skin, lung, and gastric stomach.

We used acetone-fixed frozen sections for chymase, because the routinely used Carnoy solution reduces the number of $chymase^+$ cells.[28] Antihuman chymase mAb (Chemicon, Temecula, CA) labeled slides were stained with alkaline phosphatase (AP)–conjugated 2nd Ab (Vector, Burlingame, CA). For tryptase, formalin-fixed paraffin-embedded sections and methanol-fixed cytospin preparations were incubated with antitryptase mAb (Chemicon) and with AP-conjugated 2nd Ab. The color was developed with naphthol AS-BI/new fuchsin. In some experiments, biotin-conjugated antichymase mAb-labeled cells were incubated with horseradish peroxidase–conjugated streptavidin, and the color was developed with 3-amino-9-ethylcabbazole (Vector). The cells were sequentially labeled with AP-conjugated antitryptase mAb, and the color was developed with fast blue substrate (Vector). We used healthy parts of skin obtained after mastectomy as positive controls.

For SCF distribution in NOG mouse skin, we sequentially incubated acetone-fixed frozen sections with antimouse SCF polyclonal Ab (R&D systems, Minneapolis, MN) and Cy3-conjugated 2nd Ab (Jackson) and observed with a confocal laser microscopy (Olympus).

RNA purification and RT-PCR (reverse transcription–polymerase chain reaction)

Cellular total RNA was isolated with the phenol/guanidine isothiocyanate method using a Trizol reagent (Invitrogen) and reverse-transcribed to complementary (cDNA) with oligo dT primers and SuperScript Synthesis System (Invitrogen). Reaction mixtures were amplified with 0.2 U Taq polymerase (Sigma) using 25 cycles for glyceraldehyde-3-phosphate dehydrogenase (G3PDH) and 40 cycles for others under the following conditions: denaturation at 95°C for 30 seconds, annealing at 55°C for 30 seconds, and extension at 72°C for 30 seconds. Oligonucleotide primers for SCF which recognized both human and mouse SCF, 5′-TCTTCAGCTGCTCCTATTT-3′ and 5′-ACTGCTACTGCTGTCATTC-3′; human tryptase, 5′-GGAAAACCACATTTGTGACG-3′ and 5′-ATTCACCTTGCACACAGGG-3′; and human chymase, 5′-AAGGAGAAAGCCAGCCTGACC-3′ and 5′-TCCGACCGTCCATAGGATACG-3′ were synthesized.

To evaluate the species origin of SCF, PCR products were purified with the QIAquick PCR purification kit (Qiagen, Valencia, CA) and digested for 1 hour with restriction enzymes, *Xmal* and *NsiI*. Mouse keratinocyte Pam212 and human keratinocyte DJM-1 were positive controls.

Human mast cell culture in vitro

Human cord blood $CD34^+$ cells were cultured in AIM-V medium (Invitrogen) with either human SCF (Amgen, Thousand Oaks, CA) or murine SCF (Kirin Brewery, Gunma, Japan) at concentration of 10 ng/mL (suboptimal) or 100 ng/mL (optimal), as described previously but with a minor modification.[29-31] During the first week, 50 ng/mL human IL-6 (Kirin Brewery) was also added. Flow cytometry at the constant flow rate was used to assess viable cell number with propidium iodide and mast cell percentage with anti-Kit mAb.

Statistical analysis

Data are presented as the mean ± SD values. Statistical significance was determined with the Student *t* test, and $P < .01$ was considered significant.

Results

Murine mast cell distribution in NOG mice

Compared with age-matched control B6 mice, the dermis of 12-week-old NOG mice (n = 6) has a normal concentration of mast cells (Figure 1A-B), but, surprisingly, in the skin of 20-week-old NOG mice (n = 6), we observed a substantial number of toluidine blue$^+$ cells in the upper dermis (Figure 1C-D). The pathologic findings also showed epidermal hyperplasia.

Murine mast cells collected from the peritoneal cavity were safranin$^+$ CTMCs, as from the dermis. The number of peritoneal mast cells from 12-week-old NOG mice ($0.51 \pm 0.07 \times 10^6$ cells/mouse, mean ± SD values from 6 mice) was not different from that from control B6 mice ($0.49 \pm 0.05 \times 10^6$ cells/mouse). Although peritoneal mast cells in B6 mice had a tendency to increase in number as the mice became older, 20-week-old NOG mice had significantly fewer peritoneal mast cells ($0.28 \pm 0.05 \times 10^6$ cells/mouse) than did 20-week-old B6 mice ($1.02 \pm 0.57 \times 10^6$ cells/mouse, n = 6) ($P < .01$). Figure 1E shows toluidine blue staining of the mesentery from 20-week-old NOG mice, and Figure 1F shows safranin-O staining of peritoneal cells, also from 20-week-old NOG mice.

In addition, we checked mast cells in lung and gastric tract, where MMCs were predominantly distributed. The lungs showed no mast cell at the alveoli (Figure 1G) but a few mast cells, which were safranin$^+$ CTMCs, around major airways (Figure 1H). In the gastric stomach, mast cells were distributed in both submucosa and mucosa (Figure 1I-K). Mast cells in the submucosa were safranin$^+$ CTMCs (arrowheads in Figure 1I-J), whereas unexpectedly safranin-negative, Alcian blue$^+$ MMCs were identified in gastric mucosa (arrows in Figure 1I,K), even though NOG mice lack T cells because of γ_c^{null} mutation. The number of mast cells in the lung and gastric tract of the control B6 mice and the older NOG mice had not changed.

In NOG mice, lymph nodes could hardly be identified without human HSC transplantation: only 2 lymph nodes at the axillaries and one at the mesenteric region of 6 mice. Pathologic examination of these identified lymph nodes showed a small number of mast cells located in the connective tissue at the capsule and an even smaller number of mast cells at the trabecula of the lymph node, and none in the cortex or medulla (Figure 1L). They were all safranin$^+$ CTMCs (data not shown). In spleen of NOG mice, mast cells were present in the connective tissue of the trabecula, as shown with arrows in Figure 1M. Again, they were all safranin$^+$ CTMCs (data not shown). Except for the ease of finding lymph nodes from control B6 mice, the number and histologic distribution of mast cells in lymph nodes and spleen of 12-week-old NOG mice were not different from those of the control B6 mice and the older NOG mice.

Human mast cell development in mouse skin

Four weeks after transplantation of cord blood CD34$^+$ cells, human CD45$^+$ cells were detected in NOG mouse peripheral blood, in which CD33$^+$ myeloid cells were predominant, and CD19$^+$ B cells and CD56$^+$ NK cells were also present (Figure 2). Human CD45$^+$ cells gradually increased, and 12 weeks after transplantation, we also observed abundant human CD3$^+$ T cells in NOG mice, in agreement with previous study.[18]

To identify mast cell development after human CD34$^+$ cell transplantation into NOG mice, we first tried to detect tryptase and chymase messenger RNA (mRNA) expression in the skin. Four weeks or 8 weeks after xenotransplantation (n = 3), this expression was hardly detectable. Twelve weeks after the transplantation (n = 3), however, human mast cell-specific protease expression was identified in NOG mouse skin (Figure 3A). At this time, chymase mRNA was more prominent than tryptase mRNA.

In addition, we stained skin sections with antihuman CD45 mAb, which did not react to NOG mice not receiving transplants (data not shown). Four weeks or 8 weeks after xenotransplantation (n = 3), unexpectedly we observed human CD45$^+$ cells mainly in

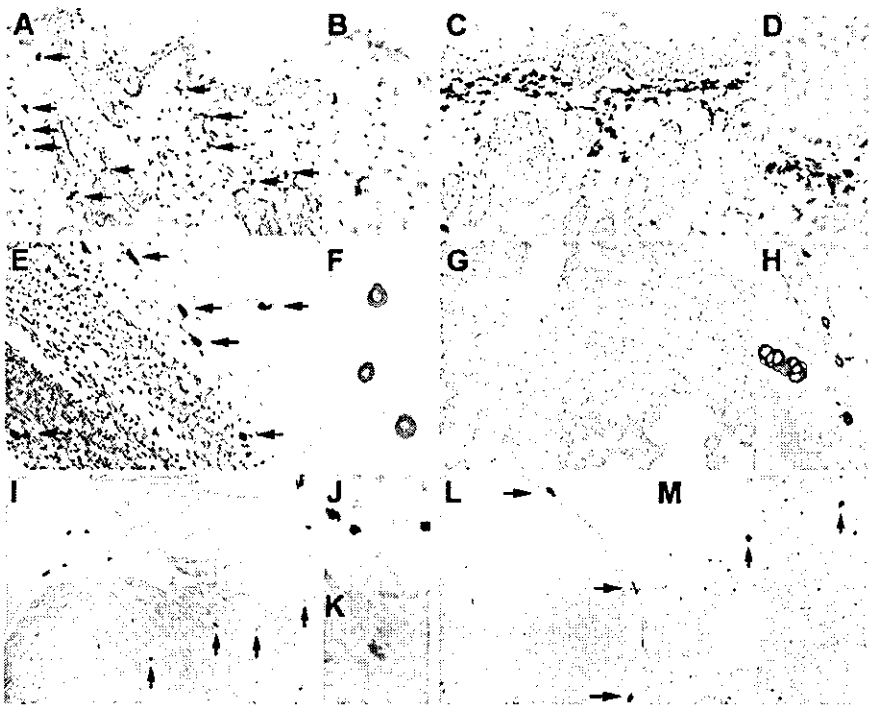

Figure 1. Murine mast cell distribution in NOG mice. (A-D) Toluidine blue staining of the skin of NOG mice. Thin frozen sections from 12-week-old (A-B) and 20-week-old (C-D) NOG mice were stained with acidic toluidine blue. Arrows in the picture from 12-week-old NOG mice (A) indicate metachromatically stained cells. The upper dermis of 20-week-old NOG mice shows bandlike proliferation of toluidine blue$^+$ cells and hyperplasia of epidermis. Magnification, × 200 (A,C) and × 400 (B,D). (E) Toluidine blue staining of mesentery of 20-week-old NOG mice, and arrows indicate mast cells. Magnification × 200. (F) Safranin-O staining of peritoneal cells obtained from 20-week-old NOG mice. Magnification, × 400. (G-K) Alcian blue and safranin-O staining in Carnoy fixed preparations from 20-week-old NOG mice. In lung, a few safranin$^+$ CTMCs were recognized around major airways (H), whereas safranin-negative, Alcian blue$^+$ MMCs were not observed in alveoli (G). In the gastric stomach, NOG mice showed safranin$^+$ CTMCs in the submucosa (arrowheads in I and image with hypermagnification in J), and safranin-negative, Alcian blue$^+$ MMCs in mucosa (arrows in I and image with hypermagnification in K). Magnification, × 100 (G,I), × 200 (H), and × 400 (J-K). (L-M) Toluidine blue staining of Carnoy fixed preparations from lymph node (L) and spleen (M) from 20-week-old NOG mice. Mast cells located only at the capsule of the lymph nodes. In the spleen, a few mast cells were present as shown with arrows in M. Magnification, × 200 (L-M).

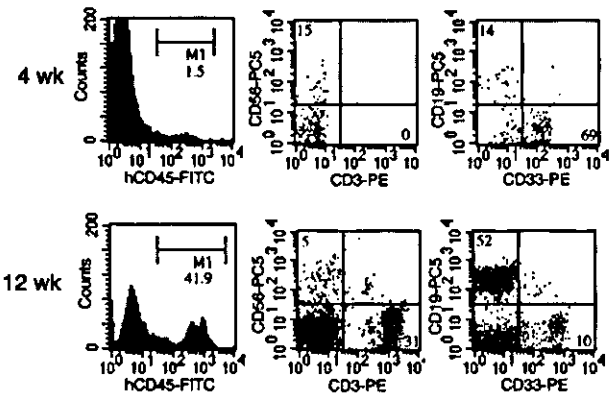

Figure 2. Representative flow cytometric analysis of peripheral blood from NOG mice after HSC transplantation. Four weeks after the transplantation, less than 2% of the cells were human CD45, in which CD33$^+$ myeloid cells were predominant, and CD19$^+$ B cells and CD56$^+$ NK cells were also present. Twelve weeks after the transplantation, more than 40% cells were replaced by human CD45$^+$ cells, among which abundant human CD3$^+$ T cells were identified.

the upper dermis and some in the basal layer of the epidermis. However, none of these human CD45$^+$ cells were positive for FITC-avidin, indicating they were not mast cells. Twelve weeks after the transplantation (n = 8), finally we could detect a small number of avidin-FITC and human CD45 double-positive mast cells in the dermis (Figure 3B). Then, the number of double-positive human mast cells gradually but focally increased to produce clusters in the dermis of NOG mice (Figure 3C).

Next, we checked the presence of human mast cell-specific tryptase and chymase by immunochemical staining. Staining the skin of NOG mice not receiving transplants with antihuman chymase mAb showed no positive cells, confirming that there was no cross-reaction to mouse mast cells (data not shown). More than 12 weeks after xenotransplantation into NOG mice, we recognized human chymase$^+$ cells focally in the dermis, and after 24 weeks (n = 6), some mast cell clusters consisted of more than 100 human chymase$^+$ cells (Figure 3D-E). The number and size of the clusters consisting of chymase$^+$ cells in NOG mouse skin differed even among the specimens obtained from the same mouse. As shown in Figure 3E, in some areas of NOG mouse skin, proliferated mast cells consisted of only chymase$^+$ human mast cells but not murine mast cells. We counted the mast cells in the area under 500 μm of skin surface and above the sebaceous gland of the dermis and found that the number of human mast cells in the area consisting of only chymase$^+$ cells (38.0 ± 8.4 cells/500 μm, mean ± SD values from 5 different preparations) and that of mouse mast cells in the area consisting of only nonstained granulated cells (39.8 ± 3.9) was almost the same 24 weeks after the transplantation (Figure 3G).

At the same time, we recognized cells showing strong positive reaction for human tryptase in the upper dermis of NOG mice on the formalin-fixed preparations. These cells were recognized only more than 12 weeks after xenotransplantation (data not shown).

Differentiation into mast cells from HSCs

To confirm de novo generation of human mast cells from HSCs, we transplanted lineage-depleted cells into NOG mice and analyzed the skin, lung, and stomach 4, 8, 12, and 20 weeks after the transplantation (n = 3 for each time point). But the time course of mast cell development in those tissues after transplantation with lin$^-$/CD34$^+$ cells was the same as that with whole CD34$^+$ cells.

Human mast cell development supported by mouse SCF

To identify what kind of environment that supports human mast cell development in NOG mouse skin, we examined SCF production. Restriction enzymes could identify the species origin of amplified PCR-products: *XmaI* cut human products to 137 and 425 base pairs (bp), whereas *NsiI* cut murine products to 257 and 305 bp (Figure 4A). Although mast cells themselves can produce SCF,[32] and we actually detected SCF derived from in vitro-cultured human mast cells, digestion of PCR products suggested that murine SCF was dominant in the skin of NOG mice even when human mast cells had been reconstituted after the successful transplantation of human CD34$^+$ cells (Figure 4B). We got the same results

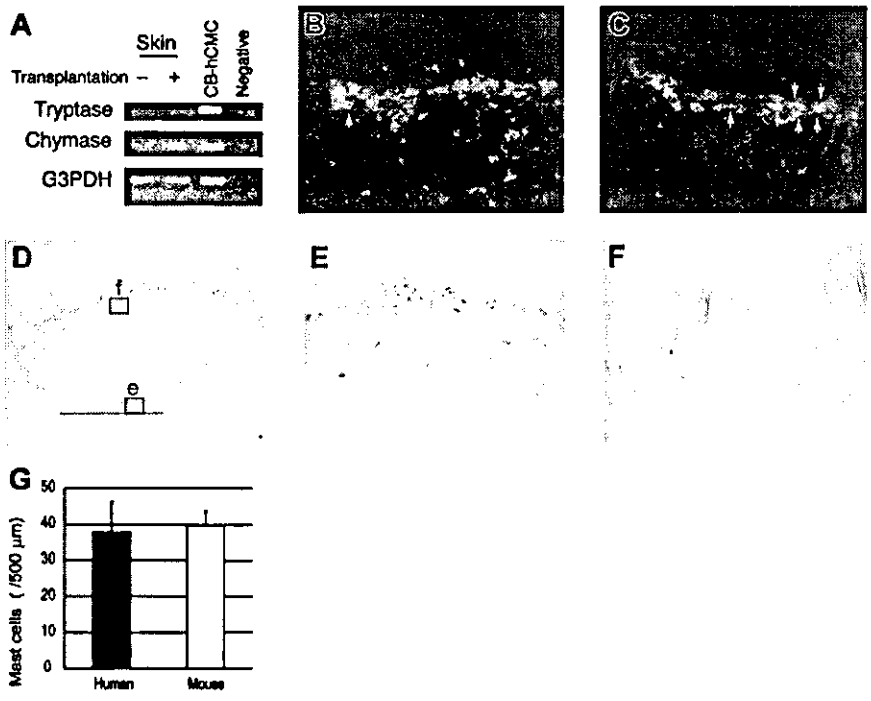

Figure 3. Human mast cell development in the mouse skin. (A) RT-PCR analysis for tryptase and chymase mRNA expression. The skin of NOG mice 12 weeks after the transplantation of human CD34$^+$ cells expressed human mast cell-specific tryptase and chymase mRNA. CB-hCMC indicates cord blood-derived human cultured mast cells. (B-C) Acetone-fixed frozen sections of NOG mouse skin 12 weeks (B) and 20 weeks (C) after the transplantation of human cord blood CD34$^+$ cells were stained for human CD45 (red fluorescent with Cy3), mast cells (yellowish green with FITC-avidin), and nuclei (blue with Hoechst 33342). Arrows indicate human CD45$^+$ mast cells, which are stained orange. Magnification, × 200. (D-F) Human MC specific chymase$^+$ cells in the mouse skin. Acetone-fixed frozen sections of NOG mouse skin 24 weeks after the transplantation were stained with antihuman chymase mAb. Human chymase$^+$ cells proliferated focally in the upper dermis (e), represented by the bar bellows, whereas in other lesions on the same samples nonstained granulated cells were located in the upper dermis (f). Magnification, × 12.5 (D) and × 200 (E-F). (G) The number of chymase$^+$ human mast cells and nonstained granulated mouse mast cells in NOG mouse skin 24 weeks after the transplantation. The number of human and mouse mast cells supported by mouse dermis was almost identical. Bar graphs display mean ± SD values from 5 different preparations.

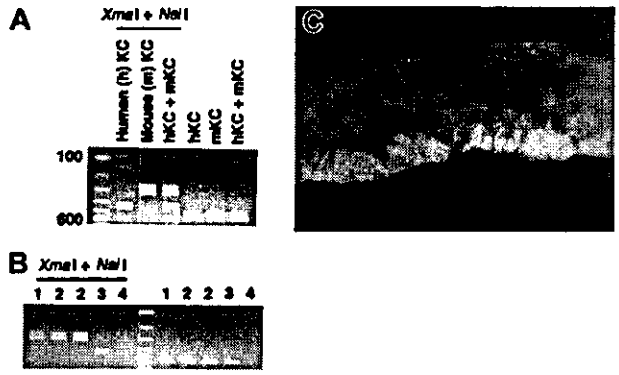

Figure 4. SCF expression in the mouse skin. (A) Control study for PCR and restriction enzymes. Templates from human DJM-1 and mouse Pam212 keratinocytes were amplified after PCR and then digested with *Xma*I and *Nsi*I. Human SCF products were cut to 137 and 425 bp and mouse SCF products to 257 and 305 bp. KC indicates keratinocytes. (B) Human mast cell development in NOG mouse skin was predominantly supported by mouse SCF. Expected 562-bp bands were observed after PCR reaction. The digestion patterns with *Xma*I and *Nsi*I suggested the main source of SCF in the skin was mouse-derived SCF even after the xenotransplantation. 1 indicates NOG mouse not receiving transplant; 2, NOG mouse 12 weeks after xenotransplantation; 3, in vitro–derived cultured human mast cells from cord blood; and 4, negative control. The findings were similar when cDNA template from NOG mouse skin was used 8 weeks and 20 weeks after the transplantation. (C) Mouse SCF protein distribution in the NOG mouse skin. SCF localized in a physiologically cytoplasmic pattern in the epidermis. Magnification × 400.

using any of the cDNA samples prepared from the NOG mice 8 weeks, 12 weeks, and 20 weeks after the xenotransplantation.

SCF has 2 phenotypes depending on its distribution pattern. It has been reported that in patients with cutaneous mastocytosis, SCF protein shifts from a cytoplasmic pattern to an intercellular pattern and represents a secretion phenotype.[33] In NOG mice, SCF was mainly produced at the epidermis where SCF localized in cytoplasm represents a physiologic phenotype (Figure 4C). This finding was similar to the findings observed before or after the transplantation of human CD34$^+$ cells into the mice.

Our result suggests that murine SCF under normal conditions supported human mast cell development in NOG mouse. We also checked whether murine SCF could support human mast cell development from cord blood by using an in vitro culture system. Six weeks after the cultivation, more mast cells had developed with murine SCF than human SCF (Figure 5), indicating that murine SCF can support human mast cell development from HSCs even more efficiently than human SCF.

Lung and gastric stomach

To determine human mast cell development in organs other than skin, we examined lung and gastric stomach, where MC_T was dominant in humans. Twelve weeks after transplantation of human cord blood CD34$^+$ cells, we could detect both tryptase and chymase mRNA in lung and gastric stomach of NOG mice (Figure 6A). In contrast to the skin, the intensity of tryptase mRNA was stronger than that of chymase mRNA in lung.

Although murine MMCs were sensitive to formalin and invisible on formalin-fixed preparations before the transplantation (data not shown), in the formalin-fixed specimens from lung 20 weeks after xenotransplantation, a small number of toluidine blue$^+$ cells, 3 to 12 cells, was observed in the frontal section of the unilateral lung (n = 4). In sequential sections, we confirmed most of the toluidine blue$^+$ cells were strongly positive for human tryptase. Human chymase$^+$ cells were seen only in the connective tissue around major airways (Figure 6B) and in the submucosal tissue under the esophagus (data not shown). In gastric stomach, we could detect formalin-resistant toluidine blue$^+$ cells in both gastric mucosa and submucosa, which were identically stained by human tryptase in sequential sections (Figure 6C). However, chymase$^+$ cells were located only in submucosa where they showed focal proliferation in clusters.

Bone marrow and peripheral blood

Although neither tryptase$^+$ cells nor toluidine blue$^+$ cells could be detected on smear preparations periodically obtained from bone marrow and peripheral blood (data not shown), analysis of more than 20 000 cells by flow cytometry identified a small number of CD203c$^+$ cells in human CD45$^+$ cells from the bone marrow (3.4% in human CD45$^+$ cells) and peripheral blood (1.2% in human CD45$^+$ cells) 20 weeks after the xenotransplantation (Figure 7A). In bone marrow, most of these CD203c$^+$ cells also strongly expressed Kit (CD117), suggesting they were human mast cells. A small portion of Kit-negative and IL-3 receptor α-chain (CD123) weakly positive cells were also observed in CD203c$^+$ cells, suggesting the presence of human basophils. However, all CD203c$^+$ cells in the peripheral blood were negative for Kit but expressed IL-3 receptor, indicating that human basophils were reconstituted from the transplanted human CD34$^+$ cells and circulated in NOG mice (n = 4).

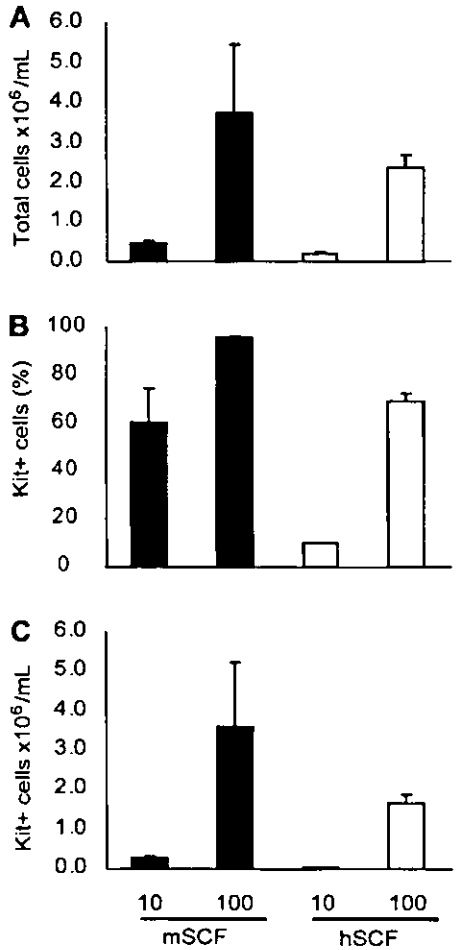

Figure 5. Mouse SCF effectively supports human mast cell development in vitro. Human cord blood CD34$^+$ cells were cultured with suboptimal (10 ng/mL) and optimal (100 ng/mL) doses of recombinant SCF. The number of mast cells (C) after 6 weeks of culture was assessed in terms of the total number of the viable cells (A) and the Kit$^+$ percentage (B) determined by flow cytometric analysis. Bar graphs display mean ± SD values from 3 independent experiments.

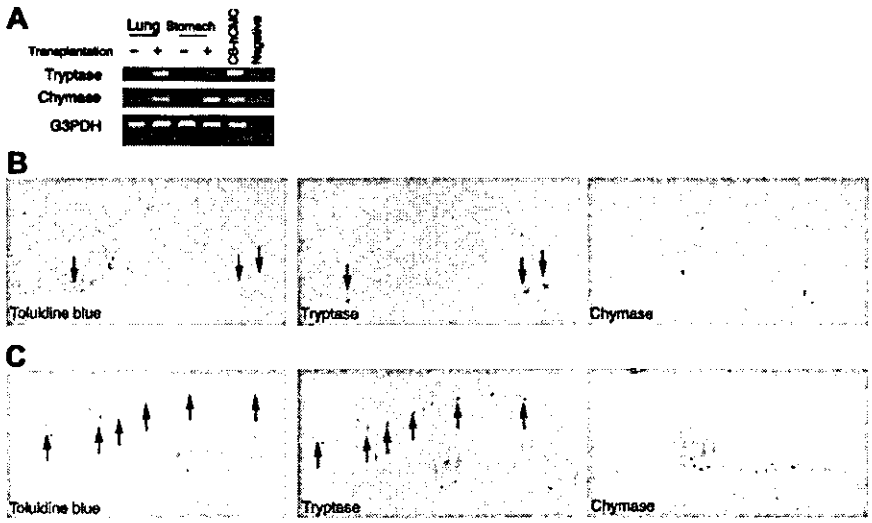

Figure 6. Human mast cell development in the mouse lung and gastric stomach. (A) RT-PCR analysis for tryptase and chymase mRNA expression. The lung and gastric stomach of NOG mice after the transplantation of human CD34$^+$ cells expressed human mast cell-specific tryptase and chymase mRNA. CB-hCMC indicates cord blood-derived human cultured mast cells. (B-C) Histologic findings for lung (B) and gastric stomach (C). Very small numbers of formalin-resistant toluidine blue$^+$ cells appeared in the lung 20 weeks after the transplantation and, in sequential sections, were almost identical to tryptase$^+$ cells (arrows). In gastric stomach, formalin-resistant toluidine blue$^+$ cells were identified in both the mucosa and submucosa. In the acetone-fixed frozen thin sections stained with antichymase mAb, chymase$^+$ cells (white arrowheads) were located only in submucosal lesions. Magnification, ⁄ 200 (toluidine blue and tryptase) and × 100 (chymase).

Peritoneal cavity and mesentery

The 2.1 ± 0.5 × 10^6 cells collected from the NOG mouse peritoneal cavity 20 weeks after the transplantation contained 3.9% ± 1.2% safranin$^+$ CTMCs (n = 4). On the cytospin preparation from the collected peritoneal cells, we failed to detect chymase$^+$ human mast cells (data not shown). Flow cytometry showed that less than 0.9% of the collected peritoneal cells expressed human CD45 (Figure 7C). Among these human CD45$^+$ cells, 2.1% expressed CD203c (0.02% of all peritoneal cells), which were human Kit$^+$ mast cells.

In the mesentery of NOG mice 20 weeks after the transplantation, we recognized a small number of human mast cell clusters consisting of 2 to 6 chymase$^+$ cells (Figure 8A).

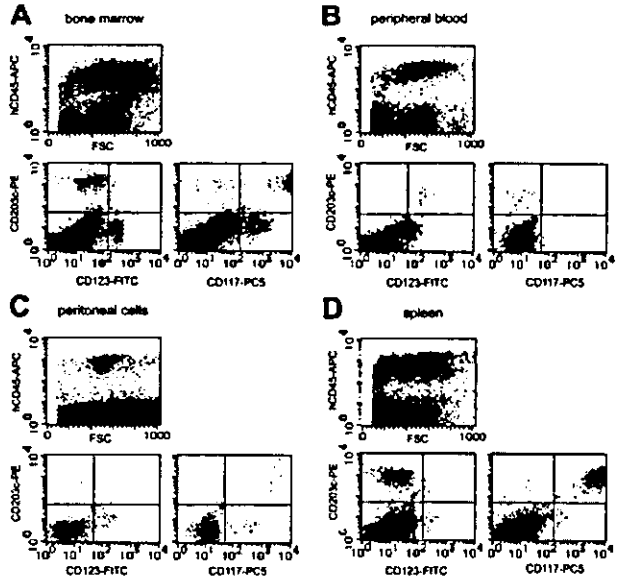

Figure 7. Representative flow cytometric analysis of bone marrow, peripheral blood, peritoneal cells, and spleen from NOG mice after HSC transplantation. Human mast cell and basophil development from the transplanted human CD34$^+$ cells were identified as CD203c/Kit (CD117) double-positive cells and CD203c/IL-3 receptor α-chain (CD123) double-positive cells, respectively, in human CD45$^+$ cells. The percentage of human CD45$^+$ cells differed depending on the transplanted cord blood-derived cells, but the proportion of CD203c/Kit double-positive cells and CD203c/CD123 double-positive cells in reconstituted human CD45$^+$ cells was similar in 4 independent experiments.

Lymph nodes and spleen

Twenty weeks after the transplantation, when human lymphocytes had already been reconstituted, only a small number of human mast cells (0 to 4 cells in the frontal section, n = 4) was identified in the lymph nodes. They were located at the trabecula and comprised human chymase$^+$ connective tissue type mast cells (Figure 8B).

Abundant human chymase$^+$ cells could be identified extensively in the red pulp but not in the white pulp of the spleen of NOG mice (n = 4) by immunochemistry (Figure 8C). These cells did not form clusters in the spleen. As shown in Figure 7D, flow cytometry confirmed the abundant presence of human mast cells as CD203c and Kit double-positive cells (9.8% in human CD45$^+$ cells and 3.3% in all spleen cells).

Discussion

Most of our studies concerning mast cells have used rodent cells. However, rodent and human mast cells show lots of heterogeneities.[34] Their dependence on growth factors is different, and the contents of secretory granules are also different. In particular, both types of human mast cells located in the mucosa and submucosa contain heparin, whereas murine MMCs lack heparin, resulting in their sensitivity to formalin. Thus, rodent mast cells are not always a suitable model for studying mast cells under the physiologic and pathologic condition in humans. The established SCF-dependent human mast cell cultures from HSCs in cord blood,[29,30,35] fetal liver,[31,36] peripheral blood, and bone marrow[37] provide new opportunities for mast cell research. By using in vitro–cultured human mast cells, we have been able to identify several new aspects of human mast cells, for example, the effect of IL-4 on human mast cells.[38-40] We also hypothesized that human mast cells participate in tissue remodeling by releasing fibrosis-induced mediators and cytokines[41] as well as produce enzymes which degenerate the extracellular matrix, known as metalloproteases.[42] However, to study the functional roles and developmental mechanism of mast cells in humans, the establishment of an appropriate in vivo model was needed.

In the study presented here we show for the first time human mast cell development in mice after xenotransplantation. Twenty weeks after xenotransplantation, we noticed the cluster formation of human mast cells, in which sometimes more than 100 human

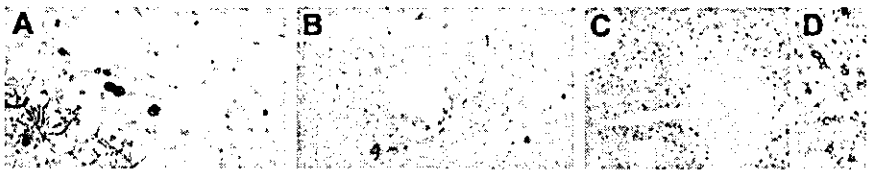

Figure 8. Immunochemical staining for human mast cell-specific chymase in mesentery, lymph nodes, and spleen. (A) In the mesentery, human mast cells formed clusters consisting of 2 to 6 chymase$^+$ cells. (B) In the lymph nodes, chymase$^+$ cells localized around vessels in the trabecula. (C-D) Abundant chymase$^+$ cells were extensively distributed in the red pulp but not in the white pulp of the spleen. Magnification, × 400 (A-B,D) and × 100 (C).

chymase$^+$ mast cells were reconstituted in the dermis of NOG mice. The question arises why human mast cells developed in NOG mice, although those derived from transplanted human HSCs have never been found in other mice. In our opinion, NOG mice have, first of all, a strong capacity for human cell engraftment, as various kinds of blood cells, including T cells, were reconstituted after xenotransplantaion.[21] Second, NOG mice may provide a suitable environment for mast cells, as dramatic mast cell proliferation was observed in the dermis of 20-week-old mice. Mast cell hyperplasia was recently reported in γδ T-cell–deficient mice with NOD background,[43] which means that mast cells in NOG mice may proliferate by being liberated from γδ T-cell regulation. The importance of the environment, which tightly regulates the number of proliferated mast cells, may also be supported by the observation that the number of mast cells in the same size area in NOG mouse skin was almost identical regardless of the origin of the proliferated mast cells.

RT-PCR analysis revealed that murine SCF made a major contribution to human mast cell development in NOG mice. Because we did not administer any human cytokines, the development of human mast cells in NOG mice indicates that SCF alone may be sufficient for human MC_{TC} development. It is also possible that some factors produced from human cells developed in mice from transplanted HSCs are synergistically involved with SCF, because human blood cells, including T cells, were reconstituted in NOG mice. Yet another possibility is that recipient mice supply some factors favorable to human mast cell development, which seems to be supported by the previous finding of an increase of human chymase$^+$ dermal mast cells after healthy human skin plantation onto SCID mice.[44]

In the spleen of NOG mice, we unexpectedly identified abundant human chymase$^+$ mast cell development, indicating that mouse spleen may provide a suitable condition for the development of human connective-tissue-type mast cells from the HSCs or committed precursors. A detailed analysis of the molecular-based mechanisms of the environment provided in the spleen should be very helpful for a better understanding of the requirement for human connective-tissue-type mast cell development.

The development of MMCs in NOG mice is of potential interest, because T-cell–derived cytokines are reportedly important for murine MMC development. Although NOG mice lack murine T cells, we found safranin-negative, Alcian blue$^+$ murine MMCs at almost normal concentrations in gastric mucosa, suggesting that factors supporting murine MMC development are produced not only by T cells.[45] Similarly, the factors required for human MC_T development remain unclear. Although some factors produced by reconstituted human T cells or other human progenies may support MC_T development in NOG mice, another possibility is that SCF is sufficient for mucosal-type mast cell development in humans. In mice, parasite infection induces reactive MMC proliferation depending on the action of IL-3,[46,47] so that parasite infection of NOG mice which have undergone xenotransplantation may provide more information about human MC_T development.

The absence of phenotypically identified mast cells on the smear preparations and CD203c/Kit double-positive cells analyzed by flow cytometry in peripheral blood indicates that human mast cells develop from immature cells without a characteristic phenotype and that their complete differentiation into mature mast cells takes place only after they have migrated to peripheral tissues. This hypothesis seems to be supported by cluster formation of human mast cells in NOG mice. Human mast cell development from contaminated precursors is unlikely, because the time course of human mast cell appearance in NOG mice that received transplants of lin$^-$/CD34$^+$ cells was not different from mice that received transplants of whole CD34$^+$ cells. Whether immature cells circulating in the peripheral blood are either already committed to becoming mast cells or maintain their capability to differentiate into other lineages than mast cells is an interesting subject for further studies.

In this study, we established for the first time an in vivo model for human mast cell development. Not only human connective tissue-type MC_{TC} but also human mucosal-type MC_T can develop in NOG mice. Our model, thus, provides useful information about human mast cell development from HSCs in vivo. In addition, this model may also pave the way to a potential tool for the in vivo investigation of human mast cell functions.

Acknowledgments

We thank Drs Atsushi Otsuka and Yukiko Tamaki (Department of Dermatology, Kyoto University) for their technical assistance and Dr Akane Tanaka (Department of Veterinary Clinic, Tokyo University of Agriculture and Technology) and Dr Michiyo Kambe (Department of Clinical Pathology, Kyoto University) for helpful discussion and advice. Language assistance was provided by Jan K. Visscher.

References

1. Williams CM, Galli SJ. The diverse potential effector and immunoregulatory roles of mast cells in allergic disease. J Allergy Clin Immunol. 2000; 105:847-859.
2. Galli SJ, Wershil BK. The two faces of the mast cell. Nature. 1996;381:21-22.
3. Nakahata T, Kobayashi T, Ishiguro A, et al. Extensive proliferation of mature connective-tissue type mast cells in vitro. Nature. 1986;324: 65-67.
4. Tsuji K, Nakahata T, Takagi M, et al. Effects of interleukin-3 and interleukin-4 on the development of "connective tissue-type" mast cells: interleukin-3 supports their survival and interleukin-4 triggers and supports their proliferation synergistically with interleukin-3. Blood. 1990;75:421-427.
5. Irani AA, Schechter NM, Craig SS, DeBlois G, Schwartz LB. Two types of human mast cells that have distinct neutral protease compositions. Proc Natl Acad Sci U S A. 1986;83:4464-4468.
6. Irani AM, Bradford TR, Kepley CL, Schechter NM, Schwartz LB. Detection of MCT and MCTC types of human mast cells by immunohistochemistry using new monoclonal anti-tryptase and anti-chymase antibodies. J Histochem Cytochem. 1989; 37:1509-1515.
7. Saito H, Hatake K, Dvorak AM, et al. Selective differentiation and proliferation of hematopoietic cells induced by recombinant human interleukins. Proc Natl Acad Sci U S A. 1988;85:2288-2292.

8. Gebhardt T, Seilge G, Lorentz A, Raab R, Manns MP, Bischoff SC. Cultured human intestinal mast cells express functional IL-3 receptors and respond to IL-3 by enhancing growth and IgE receptor-dependent mediator release. Eur J Immunol. 2002;32:2308-2316.
9. Furitsu T, Saito H, Dvorak AM, et al. Development of human mast cells in vitro. Proc Natl Acad Sci U S A. 1989;86:10039-10043.
10. Kitamura Y, Shimada M, Hatanaka K, Miyano Y. Development of mast cells from grafted bone marrow cells in irradiated mice. Nature. 1977; 268:442-443.
11. Kitamura Y, Matsuda H, Hatanaka K. Clonal nature of mast-cell clusters formed in W/Wv mice after bone marrow transplantation. Nature. 1979; 281:154-155.
12. Mosier DE, Gulizia RJ, Baird SM, Wilson DB. Transfer of a functional human immune system to mice with severe combined immunodeficiency. Nature. 1988;335:256-259.
13. McCune JM, Namikawa R, Kaneshima H, Shultz LD, Lieberman M, Weissman IL. The SCID-hu mouse: murine model for the analysis of human hematolymphoid differentiation and function. Science. 1988;241:1632-1639.
14. Ueda T, Tsuji K, Yoshino H, et al. Expansion of human NOD/SCID-repopulating cells by stem cell factor, Flk2/Flt3 ligand, thrombopoietin, IL-6, and soluble IL-6 receptor. J Clin Invest. 2000;105: 1013-1021.
15. Greiner DL, Shultz LD, Yates J, et al. Improved engraftment of human spleen cells in NOD/LtSz-scid/scid mice as compared with C.B-17-scid/scid mice. Am J Pathol. 1995;146:888-902.
16. Koyanagi Y, Tanaka Y, Tanaka R, et al. High levels of viremia in hu-PBL-NOD-scid mice with HIV-1 infection. Leukemia. 1997;11(suppl 3):109-112.
17. Yoshino H, Ueda T, Kawahata M, et al. Natural killer cell depletion by anti-asialo GM1 antiserum treatment enhances human hematopoietic stem cell engraftment in NOD/Shi-scid mice. Bone Marrow Transplant. 2000;26:1211-1216.
18. Ito M, Hiramatsu H, Kobayashi K, et al. NOD/SCID/gamma$_c^{null}$ mouse: an excellent recipient mouse model for engraftment of human cells. Blood. 2002;100:3175-3182.
19. Kollet O, Peled A, Byk T, et al. beta2 microglobulin-deficient (B2m^{null}) NOD/SCID mice are excellent recipients for studying human stem cell function. Blood. 2000;95:3102-3105.
20. Christianson SW, Greiner DL, Hesselton RA, et al. Enhanced human CD4$^+$ T cell engraftment in beta2-microglobulin-deficient NOD-scid mice. J Immunol. 1997;158:3578-3586.
21. Hiramatsu H, Nishikomori R, Heike T, et al. Complete reconstitution of human lymphocytes from cord blood CD34$^+$ cells using the NOD/SCID/gamma$_c^{null}$ mice model. Blood. 2003;102:873-880.
22. Yahata T, Ando K, Nakamura Y, et al. Functional human T lymphocyte development from cord blood CD34$^+$ cells in nonobese diabetic/Shi-scid, IL-2 receptor gamma null mice. J Immunol. 2002; 169:204-209.
23. Imai T, Koike K, Kubo T, et al. Interleukin-6 supports human megakaryocytic proliferation and differentiation in vitro. Blood. 1991;78:1969-1974.
24. Buhring HJ, Seiffert M, Giesert C, et al. The basophil activation marker defined by antibody 97A6 is identical to the ectonucleotide pyrophosphatase/phosphodiesterase 3. Blood. 2001;97:3303-3305.
25. Buhring HJ, Simmons PJ, Pudney M, et al. The monoclonal antibody 97A6 defines a novel surface antigen expressed on human basophils and their multipotent and unipotent progenitors. Blood. 1999;94:2343-2356.
26. Bergstresser PR, Tigelaar RE, Tharp MD. Conjugated avidin identifies cutaneous rodent and human mast cells. J Invest Dermatol. 1984;83:214-218.
27. Bussolati G, Gugliotta P. Nonspecific staining of mast cells by avidin-biotin-peroxidase complexes (ABC). J Histochem Cytochem. 1983;31:1419-1421.
28. KleinJan A, Godthelp T, Blom HM, Fokkens WJ. Fixation with Carnoy's fluid reduces the number of chymase-positive mast cells: not all chymase-positive mast cells are also positive for tryptase. Allergy. 1996;51:614-620.
29. Nakahata T, Tsuji K, Tanaka R, et al. Synergy of stem cell factor and other cytokines in mast cell development. In: Kitamura Y, Yamamoto S, Galli SJ, eds. Biological and Molecular Aspects of Mast Cell and Basophil Differentiation and Function. New York: Elsevier Science Publishers; 1995:13-24.
30. Saito H, Ebisawa M, Tachimoto H, et al. Selective growth of human mast cells induced by Steel factor, IL-6, and prostaglandin E2 from cord blood mononuclear cells. J Immunol. 1996;157:343-350.
31. Kambe N, Kambe M, Chang HW, et al. An improved procedure for the development of human mast cells from dispersed fetal liver cells in serum-free culture medium. J Immunol Methods. 2000;240:101-110.
32. Zhang S, Anderson DF, Bradding P, et al. Human mast cells express stem cell factor. J Pathol. 1998;186:59-66.
33. Longley BJ Jr, Morganroth GS, Tyrrell L, et al. Altered metabolism of mast-cell growth factor (c-kit ligand) in cutaneous mastocytosis. N Engl J Med. 1993;328:1302-1307.
34. Irani AM, Schwartz LB. Mast cell heterogeneity. Clin Exp Allergy. 1989;19:143-155.
35. Mitsui H, Furitsu T, Dvorak AM, et al. Development of human mast cells from umbilical cord blood cells by recombinant human and murine c-kit ligand. Proc Natl Acad Sci U S A. 1993;90: 735-739.
36. Irani AM, Nilsson G, Miettinen U, et al. Recombinant human stem cell factor stimulates differentiation of mast cells from dispersed human fetal liver cells. Blood. 1992;80:3009-3021.
37. Valent P, Spanblochl E, Sperr WR, et al. Induction of differentiation of human mast cells from bone marrow and peripheral blood mononuclear cells by recombinant human stem cell factor/kit-ligand in long-term culture. Blood. 1992;80:2237-2245.
38. Toru H, Eguchi M, Matsumoto R, Yanagida M, Yata J, Nakahata T. Interleukin-4 promotes the development of tryptase and chymase double-positive human mast cells accompanied by cell maturation. Blood. 1998;91:187-195.
39. Toru H, Kinashi T, Ra C, Nonoyama S, Yata J, Nakahata T. Interleukin-4 induces homotypic aggregation of human mast cells by promoting LFA-1/ICAM-1 adhesion molecules. Blood. 1997;89: 3296-3302.
40. Toru H, Ra C, Nonoyama S, Suzuki K, Yata J, Nakahata T. Induction of the high-affinity IgE receptor (Fc epsilon RI) on human mast cells by IL-4. Int Immunol. 1996;8:1367-1373.
41. Kanbe N, Kurosawa M, Nagata H, Yamashita T, Kurimoto F, Miyachi Y. Production of fibrogenic cytokines by cord blood-derived cultured human mast cells. J Allergy Clin Immunol. 2000;106:S85-90.
42. Kanbe N, Tanaka A, Kanbe M, Itakura A, Kurosawa M, Matsuda H. Human mast cells produce matrix metalloproteinase 9. Eur J Immunol. 1999; 29:2645-2649.
43. Girardi M, Lewis J, Glusac E, et al. Resident skin-specific gammadelta T cells provide local, nonredundant regulation of cutaneous inflammation. J Exp Med. 2002;195:855-867.
44. Christofidou-Solomidou M, Longley BJ, Whitaker-Menezes D, Albelda SM, Murphy GF. Human skin/SCID mouse chimeras as an in vivo model for human cutaneous mast cell hyperplasia. J Invest Dermatol. 1997;109:102-107.
45. Luger TA, Wirth U, Kock A. Epidermal cells synthesize a cytokine with interleukin 3-like properties. J Immunol. 1985;134:915-919.
46. Madden KB, Urban JF Jr, Ziltener HJ, Schrader JW, Finkelman FD, Katona IM. Antibodies to IL-3 and IL-4 suppress helminth-induced intestinal mastocytosis. J Immunol. 1991;147:1387-1391.
47. Lantz CS, Boesiger J, Song CH, et al. Role for interleukin-3 in mast-cell and basophil development and in immunity to parasites. Nature. 1998; 392:90-93.

Brief report

Early-onset sarcoidosis and *CARD15* mutations with constitutive nuclear factor-κB activation: common genetic etiology with Blau syndrome

Nobuo Kanazawa, Ikuo Okafuji, Naotomo Kambe, Ryuta Nishikomori, Mami Nakata-Hizume, Sonoko Nagai, Akihiko Fuji, Takenosuke Yuasa, Akira Manki, Yoshihiko Sakurai, Mitsuru Nakajima, Hiroko Kobayashi, Ikuma Fujiwara, Hiroyuki Tsutsumi, Atsushi Utani, Chikako Nishigori, Toshio Heike, Tatsutoshi Nakahata, and Yoshiki Miyachi

Early-onset sarcoidosis (EOS) and inheritable Blau syndrome (BS) share characteristic clinical features of juvenile-onset systemic granulomatosis syndrome that mainly affects skin, joints, and eyes. However, no direct evidence has been shown for the possible common origin of these 2 diseases. Recent discovery of *CARD15* mutations in BS families encouraged us to investigate similar *CARD15* mutations in EOS patients. Among 10 EOS cases retrospectively collected in Japan, heterozygous missense mutations were found in 9 cases; 4 showed a 1000C>T (R334W in amino acid change) that has been reported in BS, 4 showed novel 1487A>T (H496L), 1538T>C (M513T), 1813A>C (T605P), and 2010C>A (N670K), and 1 case showed double 1146C>G (D382E)/1834G>A (A612T) mutations on different alleles. All 6 of these variants of CARD15 showed increased basal nuclear factor (NF)–κB activity. These findings indicate that the majority of EOS and BS cases share the common genetic etiology of *CARD15* mutations that cause constitutive NF-κB activation. (Blood. 2005;105: 1195-1197)

Introduction

Sarcoidosis is a multiorganic inflammatory disease with unknown etiology, characterized by the histologic features of noncaseating epithelioid granulomas. In childhood, 2 distinct types of sarcoidosis have been described.[1] Usually the disease is detected in older children by chest radiography and the clinical manifestations are characterized by a classical triad of lung, lymph node, and eye involvement, similar to those in adults. In contrast, early-onset sarcoidosis (EOS), which usually appears in those younger than 4 years of age, is quite rare and has a distinct triad of skin, joint, and eye disorders, without apparent pulmonary involvement. Compared with an asymptomatic and sometimes naturally disappearing course of the disease in older children, EOS is progressive and in many cases causes severe complications, such as blindness, joint destruction, and visceral involvement.[2]

Blau syndrome (BS), also showing early-onset granulomatous arthritis, uveitis, and skin rash, is a rare familial disease transmitted in an autosomal dominant manner.[3] By linkage analysis, the responsible locus for BS was mapped to chromosome 16,[4] in which *CARD15* has recently been identified as the susceptibility gene.[5] CARD15 (NOD2) is a member of the growing family of nucleotide-binding oligomerization domain (NOD) proteins and composed of 2 amino-terminal caspase recruitment domains (CARDs), one NOD, and carboxy-terminal leucine-rich repeats (LRRs).[6,7] While mutations in LRRs are reportedly associated with Crohn disease (CD) and psoriatic arthritis,[8-10] 3 types of missense point mutations in the NOD, 1000C>T (R334W in amino acid change), 1001G>A (R334Q), and 1405C>T (L469F), have been discovered in BS families.[5,11,12]

It has been discussed since the first report of BS whether EOS and BS are the same diseases.[13] However, no direct evidence of their common origin has been shown and confusion still remains.[14] In the first paper describing genetic abnormalities in BS, the authors recognized no *CARD15* mutation in 2 EOS patients and therefore proposed a different etiology of BS and EOS.[5] However, we have recently described a sporadic case of systemic granulomatosis syndrome with clinical features of EOS that showed the same *CARD15* mutation as detected in BS.[15] In this report, therefore, we retrospectively collected Japanese EOS cases and searched for *CARD15* mutations, to further evaluate the relationship between EOS and *CARD15* mutations.

Study design

Patients and genetic analysis

The diagnosis of EOS was confirmed by the absence of family history of granuloma-forming diseases, as well as the typical clinical and histologic

From the Departments of Dermatology, Pediatrics, and Respiratory Medicine, Graduate School of Medicine, Kyoto University, Kyoto, Japan; the Department of Internal Medicine, Holy Spirit Hospital, Nagoya, Japan; Yuasa Ophthalmic Clinic, Osaka, Japan; the Department of Pediatrics, Okayama University Medical School, Okayama, Japan; the Department of Pediatrics, Nara Medical University, Nara Kashihara, Japan; the Department of Internal Medicine II, Fukushima Medical University School of Medicine, Fukushima, Japan; the Department of Pediatrics, Tohoku University School of Medicine, Sendai, Japan; the Department of Pediatrics, Sapporo Medical University School of Medicine, Sapporo, Japan; and the Department of Dermatology, Graduate School of Medicine, Kobe University, Kobe, Japan.

Submitted August 2, 2004; accepted September 27, 2004. Prepublished online as *Blood* First Edition Paper, September 30, 2004; DOI 10.1182/blood-2004-07-2972.

N. Kanazawa and I.O. contributed equally to this work.

An Inside *Blood* analysis of this article appears in the front of this issue.

Reprints: Nobuo Kanazawa, Department of Dermatology, Graduate School of Medicine, Kyoto University, 54 Kawahara-cho, Shogoin, Sakyo-ku, Kyoto 606-8507, Kyoto, Japan; e-mail: nkanazaw@kuhp.kyoto-u.ac.jp.

The publication costs of this article were defrayed in part by page charge payment. Therefore, and solely to indicate this fact, this article is hereby marked "advertisement" in accordance with 18 U.S.C. section 1734.

features. The agreement for genetic analysis was obtained from 10 Japanese EOS patients, whose clinical information is summarized in Table 1.[15-20] Informed consent was provided according to the Declaration of Helsinki. The study was approved by the ethics committees of Kyoto University and the organizations where the patients were under medical treatment. Genomic DNA was extracted from peripheral blood of the patients, and all 12 exons of the *CARD15* gene including exon-intron boundaries were amplified by polymerase chain reaction and sequenced. Genomic DNA of 100 healthy volunteers was examined for the mutations discovered in our patients.

Generation of CARD15 mutants and NF-κB luciferase assay

The wild-type CARD15 cDNA was generated from a healthy volunteer by reverse transcription–polymerase chain reaction. Each CARD15 mutant cDNA was generated using QuikChange Site-Directed Mutagenesis Kit (Stratagene, La Jolla, CA) and subcloned into p3xFLAG-CMV-14 vector (Sigma, St Louis, MO). HEK293T cells (1×10^5) were transfected with 1000 ng plasmids, containing 100 ng nuclear factor (NF)–κB reporter plasmid (pNF-κB-Luc; BD Biosciences Clontech, Palo Alto, CA), 30 ng expression construct of a CARD15 variant, 10 ng internal control for normalization of transfection efficiency (pRL-TK; Toyo Ink, Tokyo, Japan), and the corresponding mock vector, using *Trans*IT-293 Transfection Reagent (Mirus Bio, Madison, WI). The cells were cultured with or without 5 μg/ml muramyl dipeptide (MDP; Sigma) for 12 hours after transfection and measured for NF-κB activity using PicaGene Dual Luciferase Kit (Toyo Ink). Protein expression of each CARD15 variant was examined by Western blotting using anti-FLAG (8 amino acids; DYKDDDDK) M2 monoclonal antibody (Sigma).

Results and discussion

The genetic analysis of 10 EOS patients revealed 9 cases with heterozygous missense mutations in the NOD of the *CARD15* gene. As shown in Table 1, 4 cases showed a 1000C>T (R334W), the same mutation as reported in BS, and 4 showed novel mutations, 1487A>T (H496L), 1813A>C (T605P), 2010C>A (N670K), and 1538T>C (M513T). Case 9[19] showed double mutations, a novel 1146C>G (D382E) and a known 1834G>A (A612T), which were present on different alleles as indicated by sequencing after cloning. None of these 7 mutations is identical to a reported single nucleotide polymorphism, nor was it detected by the analysis of 100 Japanese healthy volunteers except for 1834G>A of case 9. 1834G>A, which had already been reported in one CD patient,[21] was identified in 1 of 200 alleles. Only case 10, who developed huge hepatosplenomegaly since the disease onset,[20] showed no detectable mutation in *CARD15*. These results indicate that the majority of EOS cases are related to *CARD15* mutations, especially in the NOD.

CARD15 is expressed intracellularly in phagocytic cells and recognizes MDP, a component of bacterial peptidoglycan, to induce immune responses through NF-κB activation.[6,7,22,23] The BS-related *CARD15* variants reportedly show increased basal MDP-independent NF-κB activity.[24] Accordingly, the MDP-independent and -dependent NF-κB transactivation by the novel *CARD15* mutations discovered in our EOS cases was examined in vitro to define their biologic effects. At equivalent protein expression levels, 5 novel CARD15 variants (H496L, T605P, N670K, M513T, and D382E) significantly increased the basal NF-κB activity compared with the wild-type CARD15, similar to the R334W found in both BS families and our EOS cases (Figure 1A, open bars). Although the A612T showed reduced basal NF-κB activity as reported previously,[24] cotransfection of D382E and A612T increased the basal NF-κB activity (Figure 1B, open bars), indicating the dominant positive effect of the D382E in case 9. Similar dominant positive effects of other 5 mutations were observed when cotransfected with the wild-type CARD15. In contrast, addition of a maximum dose of MDP (5 μg/mL) to each CARD15 mutant further elevated the NF-κB activity up to almost the same level as the case of the wild-type CARD15 (Figure 1A-B, filled bars). Collectively, all 6 combinations of *CARD15* variants mimicking the genotype of our EOS patients showed increased basal NF-κB activity (Figure 1B, open bars) and shared the common biologic effect with the BS-related *CARD15* variants. Although the basal NF-κB activation levels of these 6 *CARD15* variants were divergent, no remarkable correlation could be observed between the basal NF-κB activity and the disease severity (Table 1).

Recently, an extensive in vitro CARD15 mutation study has revealed that P668H and I673P mutations in the C-terminal NOD region show the increased basal NF-κB activity and minimal elevation of the activity by addition of MDP.[25] Here, we found 5

Table 1. Clinical features and *CARD15* gene mutations of 10 Japanese EOS patients

Patient	Age, y/sex	Age at disease onset	Age at start of oral steroid, y	Skin rash	Uveitis	Arthritis	Lung involvement	Other symptoms	First diagnosis	*CARD15* mutations	Selected references
1	27/M	2 y	26	+	+	+	+	NP	AD	R334W	Kanazawa, Matsushima, Kambe, et al[15]
2	30/M	2 y	–	+	+	–	–	NP	AD	R334W	
3	19/F	1 y	2	+	+	+	–	Hepatosplenomegaly Parotid swelling	JRA	R334W	Sakurai, Nakajima, Kamisue, et al[16]
4	29/F	2 y	4	+	+	+	–	NP	EOS	R334W	
5	32/F	1 y	–	+	+	+	–	Kveim test positive	EOS	H496L	Shimomura, Tada, Yamamoto, et al[17]
6	7/M	7 mo	6	+	+	+	–		EOS	T605P	
7	12/F	6 mo	2	+	+	+	–	NP	EOS	N670K	Akiyama, Seno, Tada, et al[18]
8	5/M	2 y	3	+	+	+	–	Renal calcification	EOS	M513T	
9	16/F	4 y	6	+	+	+	–	NP	JRA	D382E/A612T	Ukae, Tsutsumi, Adachi, et al[19]
10	36/F	2 y	4	+	+	+	+	Hepatosplenomegaly Lymphadenopathy Kveim test positive	EOS	–	Ito, Kato, Asano, et al[20]

y indicates years; M, male; +, presence; AD, atopic dermatitis; –, absence; F, female; JRA, juvenile rheumatoid arthritis; mo, months; and NP, nothing particular.

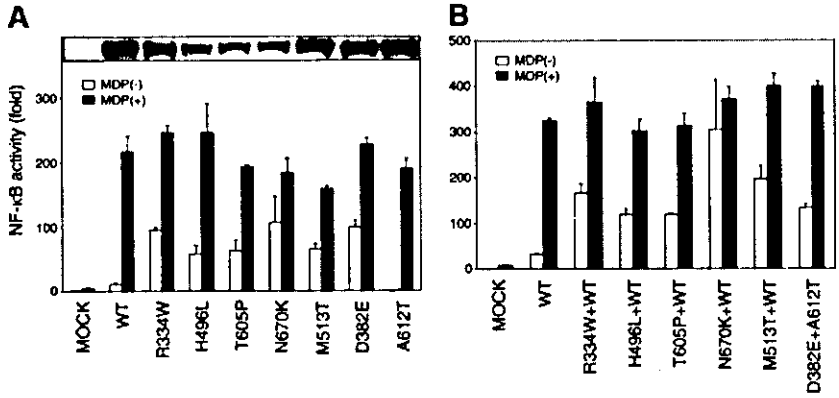

Figure 1. Biologic effects of *CARD15* variants discovered in EOS patients. (A) MDP-independent and -dependent NF-κB transactivation by *CARD15* variants discovered in EOS patients. HEK293T cells were cotransfected with 30 ng expression construct of a CARD15 variant together with the NF-κB reporter plasmid and measured for NF-κB activity after 12 hours' incubation with (■) or without (□) 5 μg/mL MDP. Mock vector and the wild-type (WT) CARD15 were used as controls. Values represent the mean of normalized data (mock without MDP = 1) of triplicate cultures, and error bars indicate SD. Shown in 1 representative result of 3 independent experiments. Protein expression levels of CARD15 variants analyzed by Western blotting are shown in the top column. (B) MDP-independent and -dependent NF-κB transactivation by combinations of *CARD15* variants mimicking the genotype of EOS patients. To reach a phenotype closer to the heterozygous *CARD15* gene expression in case 1 to 8, 15 ng of each CARD15 mutant (R334W, H496L, T605P, N670K, and M513T) was cotransfected with the same amount of the wild-type CARD15 with (■) or without (□) 5 μg/mL MDP. For case 9, 15 ng of each D382E and A612T were cotransfected. Mock vector alone and the wild-type CARD15 alone were added as controls.

novel mutations with increased basal NF-κB activity after systematic analysis of Japanese EOS cases. Indeed, location and a biologic effect of the N670K are similar to those of the P668H and I673P, but the mutations we found were distributed through the whole NOD and showed no significant difference in NF-κB activity induced by the maximum dose of MDP.

In conclusion, our results clearly show that EOS is closely related with *CARD15* mutations causing constitutive NF-κB activation and shares the common genetic etiology with BS. These findings strongly support the long-standing hypothesis that sporadic EOS and familial BS represent different types of the same juvenile systemic granulomatosis syndrome.[13]

Acknowledgments

We would like to thank Drs M. B. Lutz and T. Berger (University of Erlangen, Erlangen, Germany) for critically reviewing the manuscript.

References

1. Shetty AK, Gedalia A. Sarcoidosis: a pediatric perspective. Clin Pediatr (Phila). 1998;37:707-717.
2. Fink CW, Cimaz R. Early onset sarcoidosis: not a benign disease. J Rheumatol. 1997;24:174-177.
3. Blau EB. Familial granulomatous arthritis, iritis, and rash. J Pediatr. 1985;107:689-693.
4. Tromp G, Kuivaniemi H, Raphael S, et al. Genetic linkage of familial granulomatous inflammatory arthritis, skin rash, and uveitis to chromosome 16. Am J Hum Genet. 1996;59:1097-1107.
5. Miceli-Richard C, Lesage S, Rybojad M, et al. CARD15 mutations in Blau syndrome. Nat Genet. 2001;29:19-20.
6. Ogura Y, Inohara N, Benito A, Chen FF, Yamaoka S, Nunez G. Nod2, a Nod1/Apaf-1 family member that is restricted to monocytes and activates NF-κB. J Biol Chem. 2001;276:4812-4818.
7. Inohara N, Nunez G. NODs: intracellular proteins involved in inflammation and apoptosis. Nat Rev Immunol. 2003;3:371-382.
8. Hugot JP, Chamaillard M, Zouali H, et al. Association of NOD2 leucine-rich repeat variants with susceptibility to Crohn's disease. Nature. 2001;411:599-603.
9. Ogura Y, Bonen DK, Inohara N, et al. A frameshift mutation in NOD2 associated with susceptibility to Crohn's disease. Nature. 2001;411:603-606.
10. Rahman P, Bartlett S, Siannis F, et al. CARD15: a pleiotropic autoimmune gene that confers susceptibility to psoriatic arthritis. Am J Hum Genet. 2003;73:677-681.
11. Wang X, Kuivaniemi H, Bonavita G, et al. CARD15 mutations in familial granulomatosis syndromes: a study of the original Blau syndrome kindred and other families with large-vessel arteritis and cranial neuropathy. Arthritis Rheum. 2002;46:3041-3045.
12. Kurokawa T, Kikuchi T, Ohta K, et al. Ocular manifestations in Blau syndrome associated with a CARD15/Nod2 mutation. Ophthalmology. 2003;110:2040-2044.
13. Miller JJ. Early-onset "sarcoidosis" and "familial granulomatous arthritis (arteritis)": the same disease. J Pediatr. 1986;109:387-388.
14. James G. Blau's syndrome and sarcoidosis. Lancet. 1999;354:1035.
15. Kanazawa N, Matsushima S, Kambe N, Tachibana T, Nagai S, Miyachi Y. Presence of a sporadic case of systemic granulomatosis syndrome with a CARD15 mutation. J Invest Dermatol. 2004;122:851-852.
16. Sakurai Y, Nakajima M, Kamisue S, et al. Preschool sarcoidosis mimicking juvenile rheumatoid arthritis: the significance of gallium scintigraphy and skin biopsy in the different diagnosis. Acta Paediatrica Japonica. 1997;39:74-78.
17. Shimomura Y, Tada R, Yamamoto Y, Yuasa T. Ocular sarcoidosis in a 7-year-old child. Jap J Clin Ophthalmol. 1982;36:109-112.
18. Akiyama H, Seno A, Tada J, Arata J, Oda M. Sarcoidosis in a 6-month-old infant—report of a case and review of the literature. Jap J Dermatol. 1993;103:19-25.
19. Ukae S, Tsutsumi H, Adachi N, Takahashi H, Kato F, Chiba S. Preschool sarcoidosis manifesting as juvenile rheumatoid arthritis: a case report and a review of the literature of Japanese cases. Acta Paediatrica Japonica. 1994;36:515-518.
20. Ito S, Kato R, Asano Y, et al. A child case of sarcoidosis presenting hepatosplenomegaly. Pediatr Jap. 1977;18:613-619.
21. Lesage S, Zouali H, Cezard JP, et al. *CARD15/NOD2* mutational analysis and genotype-phenotype correlation in 612 patients with inflammatory bowel disease. Am J Hum Genet. 2002;70:845-857.
22. Inohara N, Ogura Y, Fontalba A, et al. Host recognition of bacterial muramyl dipeptide mediated through NOD2: implications for Crohn's disease. J Biol Chem. 2003;278:5509-5512.
23. Girardin SE, Boneca IG, Viala J, et al. Nod2 is a general sensor of peptidoglycan through muramyl dipeptide (MDP) detection. J Biol Chem. 2003;278:8869-8872.
24. Chamaillard M, Philpott D, Girardin SE, et al. Gene-environment interaction modulated by allelic heterogeneity in inflammatory diseases. Proc Natl Acad Sci U S A. 2003;100:3455-3460.
25. Tanabe T, Chamaillard M, Ogura Y, et al. Regulatory regions and critical residues of NOD2 involved in muramyl dipeptide recognition. EMBO J. 2004;23:1587-1597.

Impaired neutrophil maturation in truncated murine G-CSF receptor–transgenic mice

Tetsuo Mitsui, Sumiko Watanabe, Yoshihiro Taniguchi, Sachiyo Hanada, Yasuhiro Ebihara, Takeshi Sato, Toshio Heike, Masao Mitsuyama, Tatsutoshi Nakahata, and Kohichiro Tsuji

Severe congenital neutropenia (SCN) is a hematopoietic disorder characterized by neutropenia in peripheral blood and maturation arrest of neutrophil precursors in bone marrow. Patients with SCN may evolve to have myelodysplastic syndrome or acute myelocytic leukemia. In approximately 20% of SCN cases, a truncation mutation is found in the cytoplasmic region of the granulocyte colony-stimulating factor receptor (G-CSFR). We then generated mice carrying murine wild-type G-CSFR and its mutants equivalent to truncations at amino acids 718 and 731 in human G-CSFR, those were reported to be related to leukemic transformation of SCN. Although numbers of peripheral white blood cells, red blood cells, and platelets did not differ among mutant and wild-type G-CSFR transgenic (Tg) mice, both of the mutant receptor Tg mice had one third of peripheral neutrophil cell counts compared with wild-type receptor Tg mice. The mutant receptor Tg mice also showed impaired resistance to the infection with *Staphylococcus aureus*. Moreover, bone marrow of these Tg mice had an increased percentage of immature myeloid cells, a feature of SCN. This maturation arrest was also observed in in vitro cultures of bone marrow cells of truncated G-CSFR Tg mice under G-CSF stimulation. In addition, clonal culture of bone marrow cells of the truncated G-CSFR Tg mice showed the hypersensitivity to G-CSF in myeloid progenitors. Our Tg mice may be useful in the analysis of the role of truncated G-CSFR in SCN pathobiology. (Blood. 2003;101:2990-2995)

Introduction

Severe congenital neutropenia (SCN, Kostmann syndrome) is characterized by persistent neutropenia and bone marrow morphology that suggests maturation arrest of neutrophil precursors at the promyelocytic or myelocytic stage.[1] Many patients with SCN die from infectious diseases in their early life.[2] The application of granulocyte colony-stimulating factor (G-CSF) enables long time survival, but approximately 10% to 15% of the patients develop secondary myelodysplastic syndrome (MDS) and acute myelocytic leukemia (AML).[3-5] This development suggests that an impairment in the signaling pathway through the G-CSF receptor (G-CSFR) has some role in SCN.

The G-CSFR is a member of the cytokine receptor superfamily. The receptor contains extracellular, transmembrane, and cytoplasmic domains but lacks intrinsic tyrosine kinase activity. This single polypeptide forms homo-oligomeric complexes on binding to ligand and activates cytoplasmic tyrosine kinase.[6] Signal transduction pathways that involve Janus tyrosine kinases (Jak1, Jak2, and Tyk2) and signal transducer and activator of transcription proteins (STATs 1, 3, and 5) are linked to the G-CSFR.[7] Mutations have been found in the gene encoding G-CSFR in some patients with SCN.[2,4] Approximately 20% of SCN cases show similar types of molecular defects that introduce premature stop codons leading to a truncation of G-CSFR. So far, 5 types of truncation mutations have been found, which are located between nucleotides 2384 and 2429 (amino acids 716 and 731, respectively); nucleotide and amino acid numbers are based on the report by Fukunaga et al.[8] Two of them, 718 and 731 truncation mutants, were reported to be related to the transformation to MDS/AML in SCN.[2,4,9] These mutations are point mutations that result in the cytoplasmic truncation of the receptor.

A number of studies on the role of the truncated G-CSFR in SCN have been reported. McLemore et al[10] generated a mouse carrying a targeted form of these truncation mutations, using homologous recombination in embryonic stem cells. The targeted mice had normal levels of circulating neutrophils and no evidence of maturation arrest of neutrophil precursors. Hermans et al[11] simultaneously reported mice generated for the mutation in the same way as McLemore et al,[10] but their mice had reduced numbers of neutrophils in peripheral blood. Furthermore, Bernard et al[12] described that these truncation mutations were detected only in a minor percentage of transcripts in patients with SCN, and they reported a patient whose mutation spontaneously disappeared, then concluded that this gene abnormality has no role in the etiology of this disorder and is a bystander phenomenon. Thus, there has been some controversy over the involvement of truncation mutations in the pathogenesis of SCN.

To address this issue, we made 2 murine G-CSFR (mG-CSFR) truncation-mutant genes equivalent to the human 718 and 731 truncations. These fragments were inserted into the expression vector LD2 that has a promoter of the major histocompatibility complex (MHC) class I *H2Ld* gene.[13] Both types of truncation-mutant receptor-transgenic (Tg) mice had a decreased absolute

From the Division of Cellular Therapy, The Advanced Clinical Research Center, and Department of Molecular and Development Biology, The Institute of Medical Science, The University of Tokyo, Tokyo, Japan; and Departments of Pediatrics and Microbiology, Graduate School of Medicine, Kyoto University, Kyoto, Japan.

Submitted August 31, 2001; accepted December 17, 2002.

Reprints: Kohichiro Tsuji, Division of Cellular Therapy, The Advanced Clinical Research Center, The Institute of Medical Science, The University of Tokyo, 4-6-1 Shirokanedai, Minato-ku, Tokyo 108-8639, Japan; e-mail: tsujik@ims.u-tokyo.ac.jp.

The publication costs of this article were defrayed in part by page charge payment. Therefore, and solely to indicate this fact, this article is hereby marked "advertisement" in accordance with 18 U.S.C. section 1734.

neutrophil count in the peripheral blood as compared with the mice having wild-type receptors, resulting in the impaired ability to resist bacterial infection, and the bone marrow of these mutant receptor Tg mice showed an increased percentage of immature myeloid cells. These results indicate that the truncation-mutant receptor has some effect on the number of mature neutrophils. Our Tg mice may provide a good model for elucidating the role of these truncation mutations in SCN and its leukemic transformation.

Materials and methods

Constructions of mG-CSFR cDNA and the generation of Tg mice

mG-CSFR cDNA was a generous gift from Dr Shigekazu Nagata (Osaka University Medical School, Japan). Two types of truncated mG-CSFR cDNA, 717 and 730 amino acid truncations equivalent to human 718 and 731 truncations, respectively, were generated using a polymerase chain reaction (PCR) method (Figure 1), and each was inserted into the *SalI/SpeI* site of pLG1 expression vector that has a 1.4-kb mouse MHC L-locus gene (*H2-Ld*) promoter.[14] The full-length of wild-type mG-CSFR cDNA was inserted into the same vector using *SalI* and *SpeI* sites. The pLd-G-CSFR plasmids were digested with restriction enzymes, *SphI* and *XhoI* for truncated receptors and *SphI* and *NruI* for wild-type receptor, to remove the vector portion. These fragments containing *H2-Ld*–wild-type G-CSFR or –truncated receptors were separated from other fragments in low-melting agarose gel (Sea Plaque; FMC Bio Product, Rockland, ME) and purified using a QIAEX II (QIAGEN, Hilden, Germany) according to the manufacturer's instruction. Transgenes were delivered by standard oocyte injection using C57BL/6 strain.[15] The mice were maintained in microisolator cages in an environmentally controlled clean room with 12-hour light-dark cycles under specific pathogen-free conditions. Tg mice were screened for successful integration of the G-CSFR by PCR analysis of tail DNA. Mouse tail tip DNA was prepared by the removal of 1 cm tail, which was incubated in 0.5 mL lysis buffer [50 mM Tris (tris(hydroxymethyl)aminomethane)-HCl, pH 7.6, 0.1 mM EDTA (ethylenediaminetetraacetic acid), 1% sodium dodecyl sulfate, and 0.1 mg/mL proteinase K] at 55°C for 16 hours. The lysate was extracted with an equal volume of phenol and chloroform. PCR was performed using 1 μg total genomic DNA, 20 pmol primers, and 2.5 U Taq DNA polymerase (Perkin Elmer Cetus, Foster City, CA) for 30 cycles (94°C for 40 seconds, 63°C for 40 seconds, and 72°C for 40 seconds), followed by 72°C for 5 minutes using a DNA thermal cycler (Gene Amp, PCR system model 2400; Perkin Elmer). The forward primer (5′-TCATGTTATATGGAGGGGGC) was in the *H2-Ld* promoter gene, and the reverse primer (5′-GAAGATCAGGGTAACTCCAG) was in the *G-CSFR* gene. Twenty microliters of the amplified solution was electrophoresed in a 1.0% agarose gel in Tris borate EDTA (TBE) buffer and stained with 0.5 μg/mL ethidium bromide. Founder mice were bred with C57BL/6 mice to obtain progeny. In most experiments, Tg and control mice (negative littermates or age-matched non-Tg mice) were used at 6 to 12 weeks of age.

Blood cell analysis

Peripheral blood cells from 6-week-old healthy C57BL/6 mice, Tg mice, and their normal littermates were collected from the retroorbital venous plexus in glass tubes. Numbers of total white blood cells, red blood cells, and platelets and the hemoglobin concentration were determined by hemocytocounter (Cel Taq α; Nihon Kouden, Tokyo, Japan). The absolute number of peripheral blood neutrophils was calculated from the total white blood cell number, and the proportion of neutrophils that was determined on glass slide samples stained with May-Grünwald-Giemsa. Bone marrow cells from 8-week-old mice were flushed from femurs into a minimum essential medium (α-MEM; Flow Laboratories, Rockville, MD) with 2% fetal bovine serum (FBS; Hyclone, Logan, UT) using 21-gauge needles. Spleen cells were obtained by rubbing between 2 pieces of frosted glass and repeated pipetting. Cells were then passed through a 70-μm nylon cell strainer (no. 2350; Becton Dickinson Labware, Franklin Lakes, NJ). These cells were counted manually, cytocentrifuged with Cytospin 2 (Shandon, Pittsburgh, PA), and closely examined under a light microscope after staining with May-Grünwald-Giemsa for differential counting. By analysis on the cytospin samples, myeloid cells were classified into late myeloid cells, such as mature neutrophils with a banded or segmented nucleus, and early myeloid cells, such as myeloblasts, promyelocytes, myelocytes, and metamyelocytes.

To assess surface G-CSFR transgene product expression, peripheral blood mononuclear cells were incubated at 4°C for 1 hour with phycoerythrin-conjugated human G-CSF (hG-CSF) (Genzyme/Techne, Cambridge, MA), followed by flow cytometric analysis (Becton Dickinson, Mountain View, CA).

Bacterial infection

Staphylococcus aureus (*S aureus*) 18Z was grown in Luria-Bertani broth at 37°C to a late log phase, washed with phosphate-buffered saline (PBS), and stored in aliquots at −80°C until used. Stock suspension was thawed and diluted serially with PBS containing 10% (vol/vol) glycerol, then the number of viable bacteria was determined by plating on nutrient agar plates and enumerating the colony-forming unit (CFU) after overnight cultivation at 37°C. Mice were infected intraperitoneally with 1.9×10^8 *S aureus*. The dose of infection was based on the data of preliminary experiments using numbers of control mice. Survival of mice was recorded for 8 days after the infection, and the percentage of survival was calculated. The difference of survival rates among the age- and weight-matched groups was evaluated by the Kaplan-Meier log-rank test, and $P < .05$ was considered significant.

Clonal cell culture

Clonal cell culture was performed in triplicate as described.[16] Briefly, 1 mL culture mixture containing bone marrow cells (2.5×10^4 cells), α-MEM, 1.2% methylcellulose (Shinetsu Chemical, Tokyo, Japan), 30% FBS, 1% deionized fraction V bovine serum albumin (BSA; Sigma Chemical, St Louis, MO), 10^{-4} mol mercaptoethanol (Eastman Organic Chemicals, Rochester, NY), and various concentrations hG-CSF or a set of hematopoietic growth factors (mouse interleukin-3 [mIL-3], human erythropoietin [hEPO], human thrombopoietin [hTPO], mouse stem cell factor [mSCF], and hIL-6) was plated in each of 35-mm suspension culture dishes (no. 171 099; Nunc, Naperville, IL) and incubated at 37°C in a humidified atmosphere flushed with 5% CO_2 in air. Except for megakaryocytic colonies, cell aggregates consisting of more than 50 cells were scored as a colony. Colony types were determined on days 10 through 14 of incubation by in situ observation using an inverted microscope, according to the criteria of Nakahata and Ogawa.[17,18] Megakaryocytic colonies were scored as such when they had at least 4 megakaryocytes.[14] To assess the accuracy of in situ identification of colonies, individual colonies were removed with an Eppendorf micropipette under direct microscopic visualization, spread on glass slides using a cytocentrifuge, and stained with May-Grünwald-Giemsa or acetylcholine esterase for megakaryocytes.

Recombinant hG-CSF, mIL-3, hEPO, and hTPO were kindly provided by Kirin Brewery (Tokyo, Japan). mSCF was a generous gift from Amgen (Thousand Oaks, CA). hIL-6 was generously provided by Tosoh (Kanagawa, Japan). All cytokines were pure recombinant molecules and were used at concentrations that induced an optimal response in methylcellulose culture of murine hematopoietic cells. These concentrations are 100 ng/mL for mSCF, 10 ng/mL for mIL-3, 100 ng/mL for hIL-6, 2 U/mL for hEPO, and 10 ng/mL for hTPO.

Suspension culture of bone marrow cells

Bone marrow cells were incubated at an initial density of 5×10^5 cells/mL in 10% FBS-containing RPMI 1640 (Nikken Biomedical Lab, Kyoto, Japan) supplemented with or without 20 ng/mL G-CSF for 7 days. Viable cells were counted on the basis of the trypan blue dye exclusion method. To analyze morphologic features, cells were spread on glass slides and stained with May-Grünwald-Giemsa.

Results

Expression of G-CSFR in Tg mice

The murine and human G-CSFRs consist of a single chain polypeptide with 812 and 813 amino acids, respectively (Figure 1). The structure of hG-CSFR shows significant homology to that of mG-CSFR with 72.5% identity at the nucleotide level and 62.5% at the amino acid level.[19] To investigate the role of G-CSFR mutations in SCN, we made murine G-CSFR 717 and 730 truncation-mutant genes, equivalent to human 718 and 731 truncations, respectively, which were reported to be related to leukemic transformation of SCN, and we transgened them by oocyte injection using C57BL/6 mice. By PCR screening of tail tip genomic DNA, 3 founder offspring for the wild-type transgene, 7 for the 730 truncation, and 2 for the 717 truncation were found.

Surface expression of the G-CSFR transgene product in Tg mice was analyzed by flow cytometry. Mononuclear cells of peripheral blood, thymus, and spleen of the mice were gated and analyzed for their expression of G-CSFR through the binding to hG-CSF conjugated with phycoerythrin. As shown in Figure 2, offspring expressing the receptor most intensely was selected. Expression levels in peripheral blood mononuclear cells, thymocytes, and splenocytes were almost the same among transfectants. Normal littermates served as negative controls in all experiments. Expression of G-CSFR was practically of the same level in male and female Tg mice (data not shown).

Peripheral blood analysis of Tg mice

All 3 types of Tg mice had no significant difference in numbers of white blood cells, red blood cells, and platelets and similar levels of hemoglobin compared with their littermates or normal mice (data not shown). However, although no difference was found in peripheral neutrophil numbers between wild-type receptor Tg mice and their littermates, Tg mice expressing mutant 717 or 730 receptors had one third of the number of neutrophils of the respective littermates, although both littermates showed numbers comparable to normal mice (Figure 3).

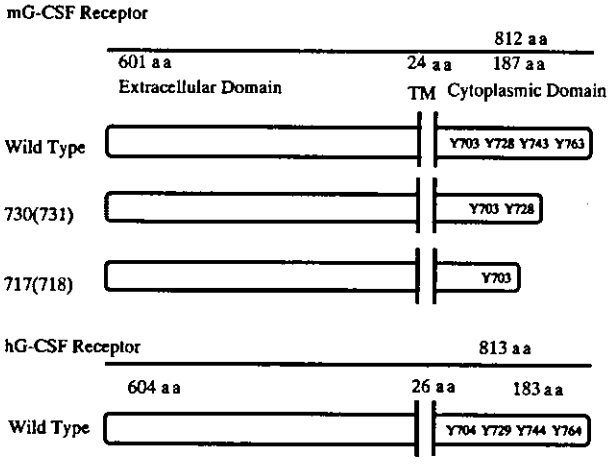

Figure 1. Schematic diagrams for the structure of murine G-CSFR, its mutants, and human G-CSFR. Murine and human G-CSFR proteins are 72.5% homologous at the nucleotide level and 62.5% homologous at the amino acid level. TM indicates transmembrane domain; Y, tyrosine residues; and aa, amino acid.

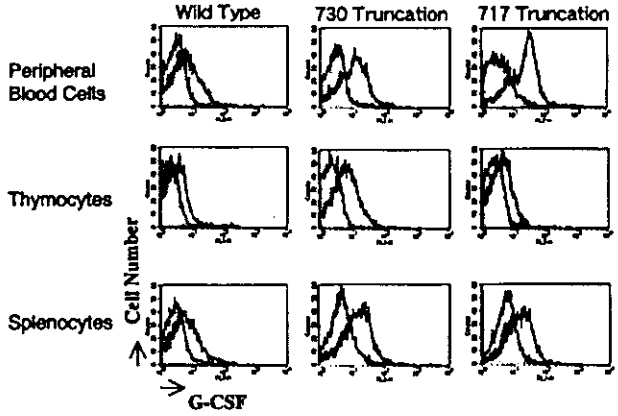

Figure 2. Expression of G-CSFR on mononuclear cells derived from Tg mice. Mononuclear cells from peripheral blood, thymocytes, and splenocytes of Tg mice carrying wild-type and mutant G-CSFR with a truncation of 730 or 717 amino acids were incubated with phycoerythrin-conjugated hG-CSF and analyzed by flow cytometry.

Bone marrow analysis of Tg mice

To elucidate the reason for the reduced neutrophils in peripheral blood of truncation receptor Tg mice, we then obtained nucleated cell counts and myelograms of bone marrow. Nucleated cell counts and the myeloid/erythroid cell (M/E) ratio had similar values in Tg mice and their littermates (Table 1). In myelogram analysis, however, percentages of early myeloid cells, such as myeloblasts, promyelocytes, myelocytes, and metamyelocytes, increased in truncation-mutant Tg mice compared with their littermates, whereas there was no difference in the distribution of myeloid cells at each stage between wild-type G-CSFR Tg mice and their littermates (Table 1; Figure 4). Thus, Tg mice expressing truncated G-CSFR showed maturation arrest at the promyelocyte to metamyelocyte stage in bone marrow, which resembles SCN, although the exclusive accumulation of promyelocytes was not observed.

Bacterial infection

To assess the susceptibility of Tg mice to bacterial infection, groups of mice were challenged with *S aureus* at a dose less than the

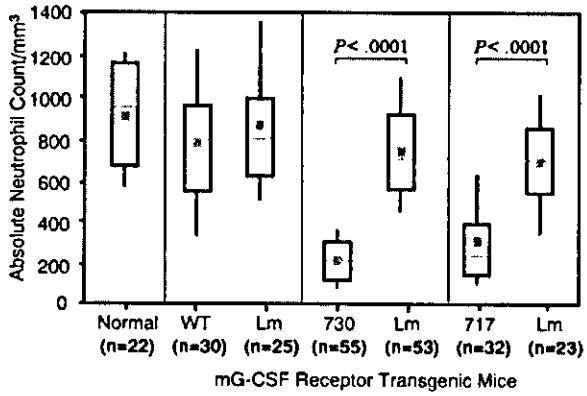

Figure 3. Box-and-Whisker plots of peripheral neutrophil counts. The top of each box denotes the third quartile and the bottom of each box denotes the first quartile. The location of the midpoint of the distribution is indicated with a horizontal line in each box. The median is indicated with a gray square. The top whisker denotes the highest 10% and the bottom whisker the lowest 10%. The Mann-Whitney *U* test was used for the statistical analysis. WT indicates wild-type G-CSFR Tg mice; 730 and 717, Tg mice expressing mutant G-CSFR with a 730 and 717 amino acid truncation, respectively; and Lm, littermates.

Table 1. Bone marrow analysis of transgenic mice

	Wild type		730 truncation		717 truncation	
	Tg, n = 3	Control, n = 3	Tg, n = 3	Control, n = 3	Tg, n = 3	Control, n = 3
NCC, 10^4/femur	2867 ± 144	2654 ± 264	2579 ± 844	2433 ± 814	2840 ± 616	2815 ± 1113
M/E ratio	1.27 ± 0.09	1.50 ± 0.38	1.17 ± 0.21	1.40 ± 0.11	1.40 ± 0.75	1.51 ± 0.20
Early myeloid, %	15.3 ± 2.43	17.43 ± 8.41	32.33 ± 3.16	19.2 ± 1.22	31.43 ± 1.26	19.87 ± 9.05
Late myeloid, %	33.57 ± 8.29	37.23 ± 1.66	14.87 ± 2.98	35.47 ± 2.0	10.77 ± 1.66	37.9 ± 8.5
Early/late ratio	0.49 ± 0.22	0.47 ± 0.24	2.21 ± 0.33	0.54 ± 0.02	2.98 ± 0.59	0.57 ± 0.35

Values indicate means ± SD; Early myeloid, immature myeloid cells at the myeloblast to metamyelocyte stage; Late myeloid, mature neutrophils with stab or segmented nucleus; NCC, nucleated cell count; M/E ratio, myeloid cells/erythroid cells ratio; and Early/late ratio, ratio of early myeloid cells to late myeloid cells.

minimum lethal dose administered to the control group (Figure 5). Death was observed within 2 days of infection in most of the groups, suggesting that *S aureus* caused an acute infection. Compared with the mortality rate in the control group, a significantly higher mortality was observed in Tg mice expressing mutant 730 (n = 7). Although a statistical significance was not obtained, Tg mice expressing mutant 717 (n = 4) showed a higher mortality as well. These data indicated that the resistance to bacterial infection was impaired in the groups of neutropenic Tg mice.

Clonal culture of bone marrow cells of Tg mice

We next examined in vitro proliferation and differentiation of hematopoietic progenitor cells in Tg mice. When bone marrow cells were cultured in methylcellulose medium containing 5 factors (mSCF, mIL-3, hTPO, hIL-6, and hEPO), no difference was found in numbers of various types of colonies, such as granulocyte-macrophage (GM) colonies, erythroid bursts, and multilineage colonies, among Tg mice and their littermates (data not shown). However, GM colony formation in response to G-CSF differed between Tg mice and their littermates or normal mice (Figure 6). When cultured with varying concentrations of G-CSF, bone marrow cells of normal mice and littermates of each Tg mouse produced similar numbers of GM colonies under sufficient G-CSF stimulation (20 ng/mL), but larger numbers of GM colonies were produced in wild-type and truncated G-CSFR Tg mice compared with their littermates ($P < .05$ in wild-type and 717 truncated receptor Tg mice) in accordance with our previous observation in hG-CSFR Tg mice.[14] Interestingly, GM colony-forming cells of wild-type and truncated G-CSFR Tg mice responded differently to G-CSF. Although the number of GM colonies gradually increased depending on the concentration of G-CSF up to 20 ng/mL in wild-type G-CSFR Tg mice as well as in normal mice and littermates of each Tg mouse, that in truncated G-CSFR Tg mice reached a plateau even at 2.5 ng/mL G-CSF, indicating a hypersensitivity to G-CSF stimulation in myeloid progenitors of truncated G-CSFR Tg mice.

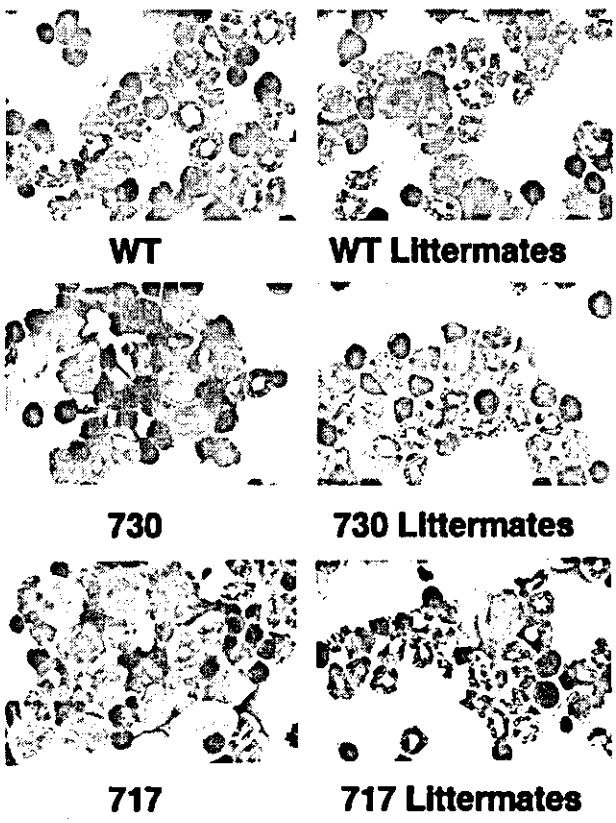

Figure 4. Morphology of bone marrow cells in Tg mice. Myeloid cells at various stages of differentiation were observed in bone marrow of wild-type (WT) G-CSFR Tg mice and littermates. In contrast, immature myeloid cells were prominent in truncation-mutant Tg mouse marrow. Original magnification × 1000; May-Grünwald-Giemsa stain.

Suspension culture of bone marrow cells of Tg mice

We also carried out suspension cultures of bone marrow cells of Tg mice. In the culture of bone marrow cells for a week with sufficient G-CSF stimulation (20 ng/mL), both truncated G-CSFR Tg mice, but not wild-type G-CSFR Tg mice, had an increased number of viable cells as compared with normal mice or their littermates (Figure 7). Morphologic analysis showed that early myeloid cells at the myeloblast to metamyelocyte stage increased in the suspension culture of truncated G-CSFR Tg mouse marrow cells, consistent with the in vivo observation (Figure 8). No obvious changes were observed in other lineages of cells, such as lymphoid cells, erythroid cells, monocytes/macrophages, and megakaryocytes.

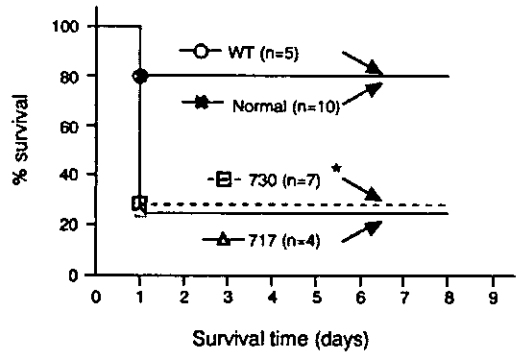

Figure 5. Survival of Tg mice to bacterial infection. Mice were infected intraperitoneally with 1.9×10^8 CFU *Staphylococcus aureus* 18Z. *$P < .05$ compared with wild-type receptor transgenic and normal mouse.

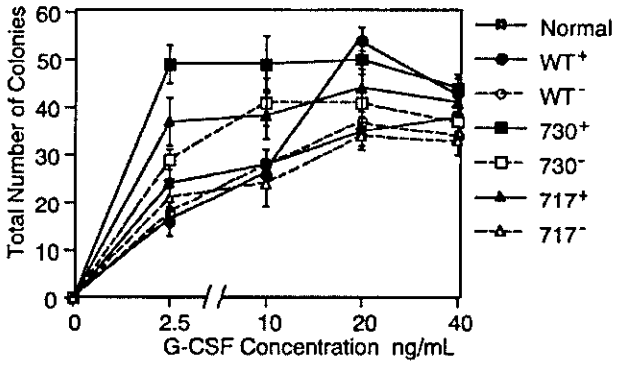

Figure 6. Dose dependence of the effect of G-CSF on colony formation. Bone marrow cells (2.5×10^4) of normal mice, Tg mice expressing wild-type G-CSFR, and mutant receptors with a 730 or 717 amino acid truncation (WT^+, 730^+, and 717^+, respectively), and their littermates (WT^-, 730^-, and 717^-, respectively) were incubated in methylcellulose culture with varying concentrations of G-CSF. Dotted lines represent littermates of the Tg mice.

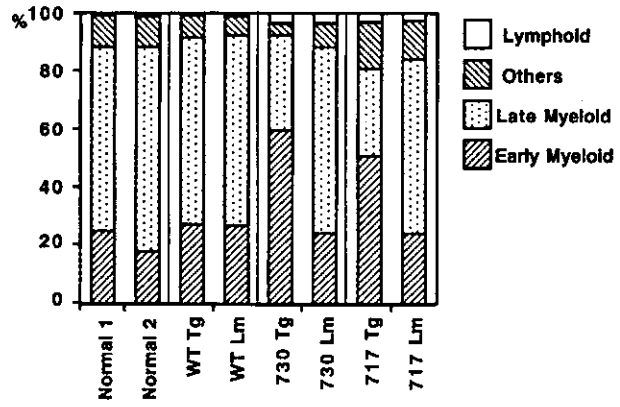

Figure 8. Differential counts of bone marrow cells in suspension culture under G-CSF stimulation. Bone marrow cells (5×10^5/mL) of normal mice, Tg mice expressing wild-type (WT) G-CSFR, and mutant receptors with 730 and 717 amino acid truncations, and their littermates (Lm) were incubated in suspension culture for a week in the presence of 20 ng/mL G-CSF. Others indicates erythroid cells, monocytes/macrophages, and megakaryocytes; Late Myeloid, mature neutrophils with a banded or segmented nucleus; and Early Myeloid, immature myeloid cell (myeloblasts to metamyelocytes). % indicates the percentage of each cell fraction in total bone marrow cells.

Discussion

To elucidate the role of G-CSFR truncations in the etiology of SCN and its leukemic transformation, we made murine G-CSFR 717 and 730 truncation-mutant transgenic mice, equivalent to human 718 and 731 truncations, respectively, which were reported to be related to leukemic transformation of SCN. Both of the generated Tg mice expressing the truncated G-CSFR showed decreased numbers of neutrophils in peripheral blood, one third of the number in wild-type receptor Tg mice, resulting in the impaired ability to resist the bacterial infection. We also observed that immature myeloid cells were predominant in bone marrow of truncated G-CSFR Tg mice. This maturation arrest of the immature myeloid cells was reproducible in in vitro culture. When stimulated by G-CSF, bone marrow cells of truncated G-CSFR Tg mice increased more than those of their littermates or wild-type G-CSFR Tg mice, but immature myeloid cells occupied a larger proportion of the increased cells. These results suggest the involvement of truncated G-CSFR in the pathogenesis of SCN. It was shown through analysis of truncated G-CSFR–transformed murine myeloid cell lines that the intracytoplasmic COOH terminal region with the domain named box 3 and 2 to 3 tyrosines among 4 is critical in myeloid differentiation, and the proximal region stimulates proliferative signals.[20-22] Therefore, signals through truncation receptors could be a negative regulator of neutrophil maturation and result in a reduced number of mature neutrophils. In the truncated G-CSFR Tg mice, the maturation arrest of myeloid cells occurred at a little later stage as compared with that in patients with SCN. It may be due to the difference in differentiation mechanism between human and murine myeloid cells. However, there may be a possibility that ubiquitous expression of receptor transgene products driven by the H2 promotor may contribute to the observed bone marrow phenotype. Primitive progenitor cells that do not normally express G-CSFR might expand as early myeloid cells.

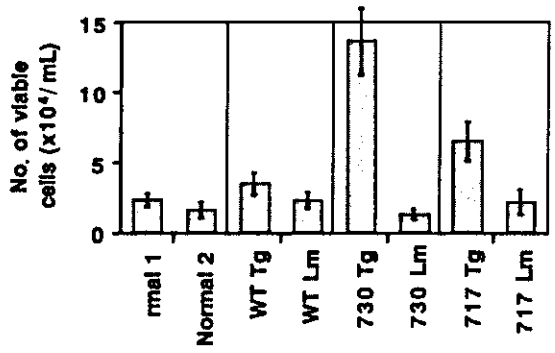

Figure 7. Total cell count in suspension culture of Tg mouse marrow under sufficient G-CSF stimulation. Bone marrow cells (5×10^5/mL) of normal mice, Tg mice expressing wild-type (WT) G-CSFR, and mutant receptors with a 730 or 717 amino acid truncation, and their littermates (Lm) were incubated in suspension culture for a week in the presence of 20 ng/mL G-CSF.

We also observed hypersensitivity of myeloid progenitors of truncated G-CSFR Tg mice to G-CSF stimulation. Consistent with the present result, 715 truncation receptor-transformed cells exhibited a hyperproliferative response to G-CSF with up-regulation of STAT5.[21-23] In addition, with sufficient G-CSF stimulation, viable myeloid cells were more abundant in suspension culture of bone marrow cells of truncated G-CSFR Tg mice than in wild-type G-CSFR Tg mice, although they had a similar number of G-CSF–responsive myeloid progenitors. Therefore, truncation-mutant receptors may be associated with prolonged myeloid cell survival under G-CSF stimulation. Thus, truncation-mutant receptors may induce proliferative stress to myeloid progenitors under thin G-CSF stimulation, and, with this proliferative stress, additional oncogenic events may act as a "second hit" for their transformation into leukemic cells.

Gene-targeted mice with a truncation of mG-CSFR reported previously showed different results to our Tg mice. The mice carrying a targeted 717 truncation mutation in the study by McLemore et al[10] have normal levels of circulating neutrophils and no evidence for a block in neutrophil maturation in bone marrow. The gene-targeted mice carrying a homozygous 715 truncation mutation in the study by Hermans et al[24] had 60% fewer circulating neutrophils but did not show maturation arrest in bone marrow. The discrepancies between the current Tg mice and previously generated Tg mice may be caused by the higher expression of transgened receptors in our Tg mice. Tidow et al[4] described 2 SCN patients with truncation mutations in the cytoplasmic domain of G-CSFR mRNA, and Kasper et al[25]

detected normal G-CSFR protein in these SCN patients. Recently, Tschan et al[26] also reported that both normal and truncated *G-CSFR* genes were detected at the same time in one patient with SCN. These reports showed that normal and truncation-mutant genes for G-CSFR exist at the same time in SCN patients with the possibility that these truncation mutations acted in a dominant-negative way. The higher levels of the truncated G-CSFR might result in a more prominent dominant-negative effect on endogenous wild-type G-CSFR. Furthermore, there may be a possibility that ubiquitous expression of truncated G-CSFR contributes to the discrepancy. Although further study should be performed, our Tg mice might be useful in the analysis of the role of truncated G-CSFR in SCN pathobiology.

Acknowledgments

We thank Imiko Hirose, Kyoko Maruyama, and Asako Hatsuyama for their expert technical assistance in the breeding and analysis of the G-CSFR Tg mice.

References

1. Kostmann R. Infantile genetic agranulocytosis. Acta Paediatr. 1956;45:1-79.
2. Dong F, Dale DC, Bonilla MA, et al. Mutations in the granulocyte colony-stimulating factor receptor gene in patients with severe congenital neutropenia. Leukemia. 1997;11:120-125.
3. Dong F, Hoefsloot LH, Schelen AM, et al. Identification of a nonsense mutation in the granulocyte-colony-stimulating factor receptor in severe congenital neutropenia. Proc Natl Acad Sci U S A. 1994;91:4480-4484.
4. Tidow N, Pilz C, Teichmann B, et al. Clinical relevance of point mutations in the cytoplasmic domain of the granulocyte colony-stimulating factor receptor gene in patients with severe congenital neutropenia. Blood. 1997;89:2369-2375.
5. Rosen RB, Kang S-J. Congenital agranulocytosis terminating in acute myelomonocytic leukemia. J Pediatr. 1979;94:406-408.
6. Demetri GD, Griffin JD. Granulocyte colony-stimulating factor and its receptor. Blood. 1991; 78:2791-2808.
7. Ward AC, Aesch YM, Gits J, et al. Novel point mutations in the extracellular domain of the granulocyte colony-stimulating factor (G-CSF) receptor in a case of severe congenital neutropenia hyporesponsive to G-CSF treatment. J Exp Med. 1999; 190:497-507.
8. Fukunaga R, Seto Y, Mizushima S, Nagata S. Three different mRNAs encoding human granulocyte colony-stimulating factor receptor. Proc Natl Acad Sci U S A. 1990;87:8702-8706.
9. Dong F, Paassen MV, Buitenen CV, Hoefsloot LH, Löwenberg B, Touw IP. A point mutation in the granulocyte colony-stimulating factor receptor (G-CSF-R) gene in a case of acute myeloid leukemia results in the overexpression of a novel G-CSF-R isoform. Blood. 1995;85:902-911.
10. McLemore ML, Poursine-Laurent J, Link DC. Increased granulocyte colony-stimulating factor responsiveness but normal resting granulopoiesis in mice carrying a targeted granulocyte colony-stimulating factor receptor mutation derived from a patient with severe congenital neutropenia. J Clin Invest. 1998;102:483-492.
11. Hermans MHA, Ward AC, Antonissen C, Karis A, Löwenberg B, Touw IP. Perturbed granulopoiesis in mice with a targeted mutation in the granulocyte colony-stimulating factor receptor gene associated with severe chronic neutropenia. Blood. 1998;92:32-39.
12. Bernard T, Gale RE, Evans JPM, Linch DC. Mutations of the granulocyte-colony stimulating factor receptor in patients with severe congenital neutropenia are not required for transformation to acute myeloid leukemia and may be a bystander phenomenon. Br J Haematol. 1998;101:141-149.
13. Yang F-C, Tsuji K, Oda A, et al. Differential effects of human granulocyte colony-stimulating factor and thrombopoietin on megakaryopoiesis and platelet function in hG-CSF receptor-transgenic mice. Blood. 1999;94:950-958.
14. Yang F-C, Watanabe S, Tsuji K, et al. Human granulocyte colony-stimulating factor (G-CSF) stimulates the in vitro and in vivo development but not commitment of primitive multipotential progenitors from transgenic mice expressing the human G-CSF receptor. Blood. 1998;92:4632-4640.
15. Hogan B, Beddington R, Constantini F, Lacy E. Manipulating the mouse embryo. New York, NY: Cold Spring Harbor; 1994.
16. Xu M-j, Tsuji K, Ueda T, et al. Stimulation of mouse and human primitive hematopoiesis by murine embryonic aorta-gonad-mesonephros-derived stromal cell lines. Blood. 1998;92:2032-2040.
17. Nakahata T, Ogawa M. Clonal origin of murine hemopoietic colonies with apparent restriction to granulocyte-macrophage-megakaryocyte (GMM) differentiation. J Cell Physiol. 1982;111:239-246.
18. Nakahata T, Ogawa M. Identification in culture of a class of hemopoietic colony-forming units with extensive capability to self-renew and generate multipotential hemopoietic colonies. Proc Natl Acad Sci U S A. 1982;79:3843-3847.
19. Avalos BR. Molecular analysis of the granulocyte colony-stimulating factor receptor. Blood. 1996; 88:761-777.
20. Fukunaga R, Ishizaka-Ikeda E, Pan C-X, Seto Y, Nagata S. Functional domains of the granulocyte colony-stimulating factor receptor. EMBO J. 1991;10:2855-2865.
21. Fukunaga R, Ishizaka-Ikeda E, Nagata S. Growth and differentiation signals mediated by different regions in the cytoplasmic domain of granulocyte colony-stimulating factor receptor. Cell. 1993;74: 1079-1087.
22. Dong F, Buitenen CV, Pouwels K, Hoefsloot LH, Löwenberg B, Touw IP. Distinct cytoplasmic regions of the human granulocyte colony-stimulating factor receptor involved in induction of proliferation and maturation. Mol Cell Biol. 1993;13: 7774-7781.
23. Dong F, Liu X, Koning JP, et al. Stimulation of Stat5 by granulocyte colony-stimulating factor (G-CSF) is modulated by two distinct cytoplasmic regions of the G-CSF receptor. J Immunol. 1998; 161:6503-6509.
24. Hermans MHA, Antonissen C, Ward AC, Mayen AEM, Ploemacher RE, Touw IP. Sustained receptor activation and hyperproliferation in response to granulocyte colony-stimulating factor (G-CSF) in mice with a severe congenital neutropenia/ acute myeloid leukemia-derived mutation in the G-CSF receptor gene. J Exp Med. 1999;189:683-691.
25. Kasper B, Herbst A, Pilz C, et al. Severe congenital neutropenia patients with point mutations in the granulocyte colony-stimulating factor (G-CSF) receptor mRNA express a normal G-CSF receptor protein [letter]. Blood. 1997;90:2839-2841.
26. Tschan CA, Pilz C, Zeidler C, Welte K, Germeshausen M. Time course of increasing numbers of mutations in the granulocyte colony-stimulating factor receptor gene in a patient with congenital neutropenia who developed leukemia. Blood. 2001;97:1882-1884.